Chapter 3

THE TITAN HAZE SIMULATION (THS) EXPERIMENT ON COSMIC PART III: EX-SITU ANALYSIS OF AEROSOLS USING DIRECT ANALYSIS IN REAL TIME MASS SPECTROMETRY (DART-MS)

3.1 Abstract

In this work, we present the results of a new ex situ diagnostic, Direct Analysis in Real Time Mass Spectrometry (DART-MS), on the solid phase samples produced in the Titan Haze Simulation (THS) experiment. This study is the next step in the analysis of the THS Titan aerosol simulants, complementing and following up on the gas phase study introducing the THS experiment (Part I) and the initial solid phase analysis by infrared (IR) spectroscopy and Scanning Electron Microscopy (SEM) (Part II). The THS experiment provides a unique simulation of Titan's atmosphere by inducing chemical reactions in N_2-CH_4-based gas mixtures over short timescales, using a pulsed plasma discharge in the stream of a jet-cooled expansion. By generating a pulsed plasma in an expanded gas, the chemistry occurs at Titan-like temperatures (~150-200K) and is truncated. The THS experiment can be tested with a range of mixtures, from N_2 and CH_4 to mixtures containing heavier molecules detected in Titan's atmosphere. The results of this study show, as expected from Part I and Part II, that the chemistry induced in the THS experiment can be considered a good analog of Titan's early and intermediate atmospheric chemistry, and allows one to study specific chemical pathways. This analysis is the first study of Titan aerosol simulants

utilizing DART-MS, and as such also allowed to demonstrate the interest of the DART technique for future analyses and preparation of future missions. This analytical technique enables the study of samples with minimal preparation or pre-processing, making it advantageous for the analysis of complex organic mixtures. The results presented here provide insight into the effects different dopant molecules, in this case benzene and acetylene, have on the aerosol products. By reviewing these effects, we can obtain a better understanding of the mechanisms that are at play within the THS experiment and possibly Titan's atmosphere.

3.2 Introduction

Since the discovery of complex organic molecules on Titan by Cassini and other missions, the synthesis and characterization of atmospheric aerosols representative of Titan has become a key research target for the astrobiology community [1-7]. Various laboratory simulation experiments have been developed to better understand Titan's atmospheric chemistry. There are four major parameters of Titan's atmosphere that need to be taken into account when simulating the chemistry: a representative gas mixture of nitrogen (90-98%) and methane (2-10%), an energy source representative of solar radiation, low pressures (in Titan's atmospheric region where photochemistry is expected to occur, the pressure can be as low as of 10^{-6}-10^{-7} mbar), and a low temperature of approximately 160-180K.[8-12] Replication of these conditions in laboratory environments is of varying difficulty, with adjustments being typical for experimental optimization. The gas mixture is the simplest factor to modify. The effect of changes on the methane/nitrogen ratio in particular have been

well characterized in prior studies.[13, 14] Pressure is the most difficult parameter to simulate accurately in the laboratory, since low pressures extend experimental time scales due to limited collisions, reduced chemistry, and slow accumulation of the aerosol, thus complicating the testing of various characterization methods. As a consequence, pressure used in laboratory experiment is often increased to higher range than Titan's atmosphere.[9, 15, 16]

The energy source used to induce chemistry is the primary origin of variability with laboratory production of Titan aerosol simulants. UV light sources are considered to be the most representative of the photochemical energy sources on Titan, but very few such sources are able to dissociate nitrogen, a key step for chemistry in Titan's atmosphere.[9] Synchrotron experiments can produce high enough energies to dissociate nitrogen but they often use a narrow bandwidth, not representative of the solar energy distribution.[17-19] The SOLEIL synchrotron experiments can generate a radiation distribution representative of the solar spectrum, but these experiments are typically performed at room temperature and have undergone limited solid phase analysis at this point.[17-20] Plasma discharge sources are used to overcome the limitations of nitrogen dissociation with UV,[15, 16, 21, 22] but introduce their own issues. The most common concern with plasma sources is the continuous reaction of the gaseous species and aerosols within the discharge region which could result in over processing of the material, since aerosol accumulation in the majority of these experiments occurs in, or close to, the plasma discharge region.[23]

The Titan Haze Simulation (THS) experiment using the COSmIC facility at the NASA Ames Research Center has previously been shown to overcome many of these concerns.[24, 25] The experiment utilizes a pulsed cold plasma discharge in a gas expansion to

generate aerosol simulants, with the ability to add other heavy molecules as desired. There are two factors that make this experimental setup unique: the use of a supersonic expansion to cool the gas mixture down to ~150 K (i.e., representative of Titan) prior to inducing the chemistry by plasma discharge, and the pulsed nature of the plasma, which limits the amount of chemical reactions occurring in the active region of the plasma discharge. This enables the analysis of the first and intermediate steps of the chemistry, as well as the examination of specific chemical pathways. Aerosols are produced in the plasma expansion and then deposited on a substrate placed further down in the stream of the jet-cooled expansion for further ex situ analysis. The products of this experiment have been analyzed in the gas phase for nascent ions through time-of-flight mass spectrometry (TOF-MS), [24] and in the solid phase by scanning electron microcopy (SEM) for characterization of aerosol morphology, and infrared (IR) spectroscopy for identification of functional groups.[25]

Mass spectrometry is complementary to IR spectroscopy for the analysis of complex mixtures with unknown constituents, allowing for the exact identification of some species. In this work, we prioritized the detection of small (< 200 Da), polar, and volatile compounds, due to the expectation of simpler products resulting from the truncated THS chemistry, nitrogen containing molecules being astrobiologically significant, and volatiles being trapped in the solid grain matrix during slow deposition, respectively. The small molecule criteria excluded the use of methods typically well suited for complex organic mixtures, such as Matrix Assisted Laser Desorption Ionization (MALDI), due to their higher molecular weight requirements.[26-28] Gas Chromatography Mass Spectrometry (GC-MS) was not chosen as it is usually employed for non-polar compounds, although a future analysis for hydrocarbon constituents could benefit from this method.[29, 30] A pyrolysis mass

spectrometry method has recently been applied to Titan aerosol simulants produced at SOLEIL using Photoelectron Spectroscopy (PES).[20] However, while isomers were readily identified for many compounds, there are limitations to this technique from the lack of reference spectra and increased structural isomers for molecules of masses greater than 70 Da. These considerations have led to the investigation of ambient mass spectrometry techniques for the analysis of the THS samples.

Ambient mass spectrometry comprises a wide range of analytical methodologies by which analyte ions can be produced at atmospheric pressure and then transferred to the vacuum region of a mass spectrometer for subsequent analysis.[31, 32] Ionization methods utilizing ambient mass spectrometry have the benefits of preserving more volatile compounds and being well suited for the analysis of polar molecules. The most common ambient ionization method is electrospray ionization (ESI), a solvent based method. ESI has been used for the analysis of Titan aerosol simulants produced in prior work and allows for the analysis of species up to 2000 Da.[14, 27] The use of solvent based methods for Titan simulant analysis is complicated due to incomplete solvation of the sample in solvents suitable for ESI.[26] Additionally, the preparation of the sample can lead to the loss of volatile constituents of interest. Plasma based ambient mass spectrometry has been developed more recently and has been utilized for a wide variety of samples.[33] One particular method, direct analysis in real time (DART), has been successful in the analysis of petroleum samples and simulated organic aerosol.[34-36] For that reason, DART was selected as the ambient ionization method for this study. It is the first time a Titan aerosol simulant has been analyzed with this technique.

As with many ambient mass spectrometric ionization methods, DART performs both desorption of the sample into the gas phase and ionization of the analytes.[37] DART utilizes a corona discharge to produce helium metastables. Upon collision with atmospheric water these metastables create protonated water clusters through Penning ionization. These water clusters then undergo proton transfer with gaseous analyte molecules, desorbed as neutrals by the helium gas, before entering the mass spectrometer.[38] While this proton transfer mechanism is typically dominant, adduct formation with water and ammonia can also be observed, along with the formation of radical cations through direct Penning ionization.[39] In all DART ionization mechanisms, very little fragmentation of the analyte is observed. Additionally, gas temperature can be increased with a heater to amplify the detection of lower volatility molecules.

Detection with DART is dependent on volatility and proton affinity. This has been demonstrated by the difficulty of applying DART ionization to hydrocarbon compounds 40. Even without taking non-polar compounds into account, complex organic mixtures typically contain a variety of DART ionizable molecules. This variety of species introduces competitive ionization, previously observed with DART [41] analyses, where easily ionized molecules suppress the detection of other molecules within a mixture and consequently impact the detection of compounds with low volatilities or proton affinities. Prior studies of Titan aerosol simulants show a similar diversity of compounds with a range of volatilities and proton affinities.[35] This wide assortment of molecules could introduce similar competitive ionization concerns, impacting the detection of molecules within the simulants. However, taking into consideration the similarity between the THS simulants, Earth aerosol simulants, and petroleum samples, as well as prior successful application of DART analysis

to the latter two types of samples, the impact of competitive ionization on the analysis should be minimal for the identification of the small, volatile, and polar compounds of interest in this work.

The analysis of THS simulants by DART serves another purpose: a test of the technique's feasibility for future missions. DART is known for its ability to perform an analysis of samples without solvation or other sample processing such as pyrolysis. This implies that DART could be considered as a possible ionization method for future lander missions. To confirm this possibility, a representative Titan aerosol simulant would need to be tested. The SEM study performed on the THS aerosols[25] has shown that the THS aerosol grains are produced in the gas phase and can be jet-deposited onto a substrate for ex situ analysis, and are therefore good analogs of how Titan aerosols would be collected at high speed by a lander during atmospheric descent. This DART study of THS aerosols consequently allows not only for the testing of the DART technique on Titan aerosol simulants for characterization purposes, but also serves as a test feasibility for future missions.

We present here the EZ-DART-MS analysis of THS simulants produced from four gas mixtures, previously analyzed by SEM and IR. The EZ-DART is a home built DART source successfully used in the past in the analysis of other complex organic mixtures.[41] The DART-MS analysis presented here focuses on identifying species present in the samples, and comparing the results to both the THS IR experiments[25] and other Titan simulant studies. The possible implications of the observed compounds for Titan's atmospheric chemistry are also discussed.

3.3 Experimental

3.3.1 COSmIC THS experiment and production of Titan aerosol simulants

The THS experimental setup and the characterization by time-of-flight mass spectrometry of the gas phase chemistry occurring in the plasma have been described in detail in Part I.[24] The description of the production of solid phase samples and their analysis by IR absorption spectroscopy and SEM have been provided in Part II.[25] Here, we present a brief description of the system. The THS experiment utilizes a pulsed plasma expansion, which causes chemical reactions in a jet-cooled gas mixture. This pulsed plasma expansion is generated by a pulsed discharge nozzle (PDN), a representation of which is shown in figure 3.1. In operation, a gas mixture is continuously injected into a copper reservoir where it equilibrates before being released in 1.28ms long pulses through a 127 μm-tall by 100 mm-long slit, cut in a 4.6 mm-thick copper plate (labeled "a" in figure 3.1). This produces a planar supersonic jet expansion with adiabatic gas temperature and pressure drops, enabling cooling of the gas mixture prior to plasma chemistry without the need for other cooling methods. In the subsequent 400 μm x 100 mm slit area (labeled "b" in figure 3.1), cut in a 1.5 mm-thick alumina plate that serves as a dielectric, the pressure and temperature drop to 30 mbar and 150 K, respectively. The plasma discharge that induces the chemistry is generated within this 1.5 mm plasma cavity by applying a pulsed negative voltage (300 μs, 600 V to 1000 V) onto a set of Elkonite (90% tungsten, 10% copper) cathodes placed 400 μm apart, along the slit, on the other side of the alumina plate.

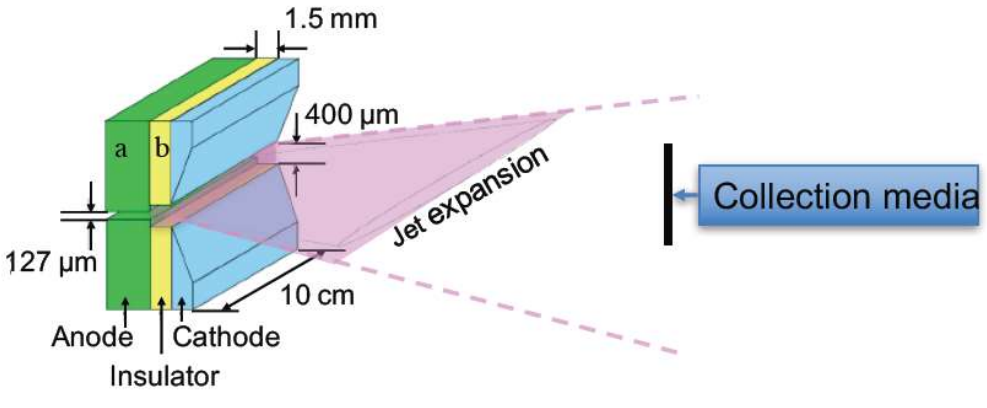

Figure 3.1. Schematics of the THS Pulsed Discharge Nozzle (PDN) and the setup for collection of solid phase samples, 5 cm away from the slit downstream of the PDN. (Schematics of the PDN adapted from Broks et al., 2005)

The characteristics of the cold plasma expansion have been evaluated both computationally and experimentally in prior studies.[25, 42, 43] These investigations have confirmed that the temperature in the plasma cavity is 150 K, without plasma activation, and around 200 K when the plasma is turned on, and remains so even with the addition of methane to the nitrogen gas mixture. In addition, because the gas is accelerated to supersonic speed in the PDN expansion, the residence time of the gas in the active region of the pulsed plasma discharge is on the order of 3 µs, allowing us to control how far the chain of chemical reactions progresses, depending on the precursors present in the initial gas mixture. This controlled or truncated chemistry minimizes concerns of over processing of the aerosols inherent to many other systems using plasma to simulate Titan's chemistry. The cold temperature and truncated chemistry facilitated by the THS experimental setup enable the study of chemical products representative of the early and intermediate stages of Titan's atmospheric chemistry. The addition of larger molecules, detected as trace elements in

Titan's atmosphere, into the initial N_2-CH_4 gas mixture allows for characterization of the effects these molecules have on the aerosol production and composition.

The gas phase experimental results, previously reported in Part I, were measured using an orthogonal reflectron time of flight mass spectrometer (reTOF-MS). For the solid phase studies presented here and in Part II, the reTOF-MS was capped off and rotated out of the chamber, and the chamber was sealed with a flange door. The deposition of the simulants onto substrates and their collection are described below. For the solid phase experiments, four gas mixtures, similar to those studied in Part I, were used to simulate different potential chemical pathways in Titan's atmospheric chemistry: N_2-CH_4 (95-5), N_2-CH_4-C_2H_2 (91-5-4, acetylene), N_2-CH_4-C_6H_6 (90-5-5, benzene), and N_2-CH_4-C_2H_2-C_6H_6 (86-5-4-5, acetylene and benzene). For each run, a ultra-high-purity (UHP, 99.9998%) N_2 gas cylinder and a UHP gas cylinder containing a N_2-CH_4 mixture with 10% + 0.2% CH_4 were used. A methane ratio of 5% was chosen for the solid phase studies (Part II and this study) instead of the 10% used in the gas phase study (Part I), in order to be more representative of Titan's atmosphere, and because the production yield is higher in the THS with 5% CH_4 than 10% CH_4. The protocols for the addition of benzene and acetylene into the N_2-CH_4-based mixtures have been fully explained in Part I. The chosen C_2H_2 and C_6H_6 concentrations are higher than the actual concentrations on Titan. This is done on purpose, in order to enhance and accelerate the chemistry and ensure that the effects of their presence on the solid phase composition are detectable, knowing that only the first and intermediate steps of the chemistry have time to occur in the THS experimental setup due to the short residence time in the plasma discharge. The goal of these experiments is to try and better understand how differences in atmospheric concentration could impact Titan's chemistry.

3.3.2 Collection of THS solid Titan aerosol simulants

The means of deposition and collection of the solid phase products have been described previously in Part II.[25] A summary is presented here. The solid samples collected from the THS experiment for analysis consist of solid grains that are produced in the plasma cavity and then jet-deposited onto a substrate placed within the expansion region approximately 5 cm downstream from the PDN. Figure 3.2c shows an example of THS deposition on aluminum foil. The interference fringes observed can be attributed to variations in deposition thickness.

The THS solid aerosols can be deposited onto different types of substrates. For this study, the THS solid samples were deposited on high vacuum aluminum foil (hv-Al). This substrate was chosen due to a large surface area and its lack of porosity, which allowed for maximum accumulation of grains. Because of the very short residence time of the gas in the plasma cavity and the resulting truncated chemistry, very small amounts of aerosols are produced in the THS experiment, even when adding larger molecules to the initial mixture.[25] As a result, it is necessary to run the experiment for several hours in order to accumulate sufficient material on the substrate for a successful ex-situ analysis. The accumulation time varies depending on the gas mixture, with the more complex mixtures producing material faster.[25] The timescales used for the present analysis were the same as the ones used for the IR ex situ analysis presented in Part II, enabling a comparison between the two studies: 10 hours of deposition were sufficient for complex mixtures containing acetylene and/or benzene, while 40 hours were necessary for the N_2-CH_4 (95-5) mixture. To ensure that the

choice of aluminum foil as a substrate did not lead to thermally induced chemical changes, temperature was monitored in blank runs using a K-type thermocouple and no significant increases in temperature (6°C in 40 hours) were observed over the timescale of the experimental runs.

After deposition, the plasma is turned off and the COSmIC chamber is pumped down to base pressure, then returned to atmospheric pressure with pure nitrogen to minimize undesired oxygen induced chemistry. The samples are then removed from the chamber through a custom-designed glove box, as discussed in Part II. The glove box is pumped down and purged with argon three times while the oxygen content is monitored with an oxygen detector to insure it is below 0.1% prior to opening the chamber. Once the samples are removed from the chamber, they are quickly stored in hv-Al foil coated plastic petri dishes and sealed with parafilm for storage. After confirming the integrity of the seal, the samples are taken to a freezer for longer term storage and kept frozen until the chosen ex-situ analysis can be performed. For the study presented here, the samples were analyzed with DART-MS within 30 minutes of their removal from the freezer.

3.3.3 EZ-DART Source

The custom-designed EZ-DART system was developed at Caltech and has been utilized for the characterization of secondary organic aerosols and viscous asphalt samples, making it well suited to this work. Figure 3.2 shows a schematic as well as two pictures of the experimental setup for the EZ-DART system. Helium is used as the flow gas (99.995% purity) at a flow rate of 1.5 L min^{-1}. A corona discharge is used to produce helium

metastables, and is generated by applying 1.5-2 kV DC with a current of 0.1-0.2 mA onto a high voltage electrode. While an ion filter is used in typical DART studies, its use was found to negatively impact CID analyses. As such, the ion filter was not used and held at ground to prevent charge buildup. The outlet of the EZ-DART is oriented at a 45° angle from the sample with the outlet no farther than 5 mm from the sample surface, as shown in figure 3.2c. An ion transfer tube is then used to guide the analyte ions into an ion trap mass spectrometer (LTQ-XL, Thermo Scientific, San Jose, CA) for detection and analysis. If desired, the temperature of the helium gas can be increased using a variable transformer controlled (Variac Co., Cleveland, OH) heating cord (Omega Engineering, Stamford, CT) wrapped around the heating region of the EZ-DART. High temperature experiments were performed for comparison to room temperature data. In all cases the temperature was measured with a K-Type thermocouple placed between the heater and glass, with all temperatures reported within + 3°C.[41]

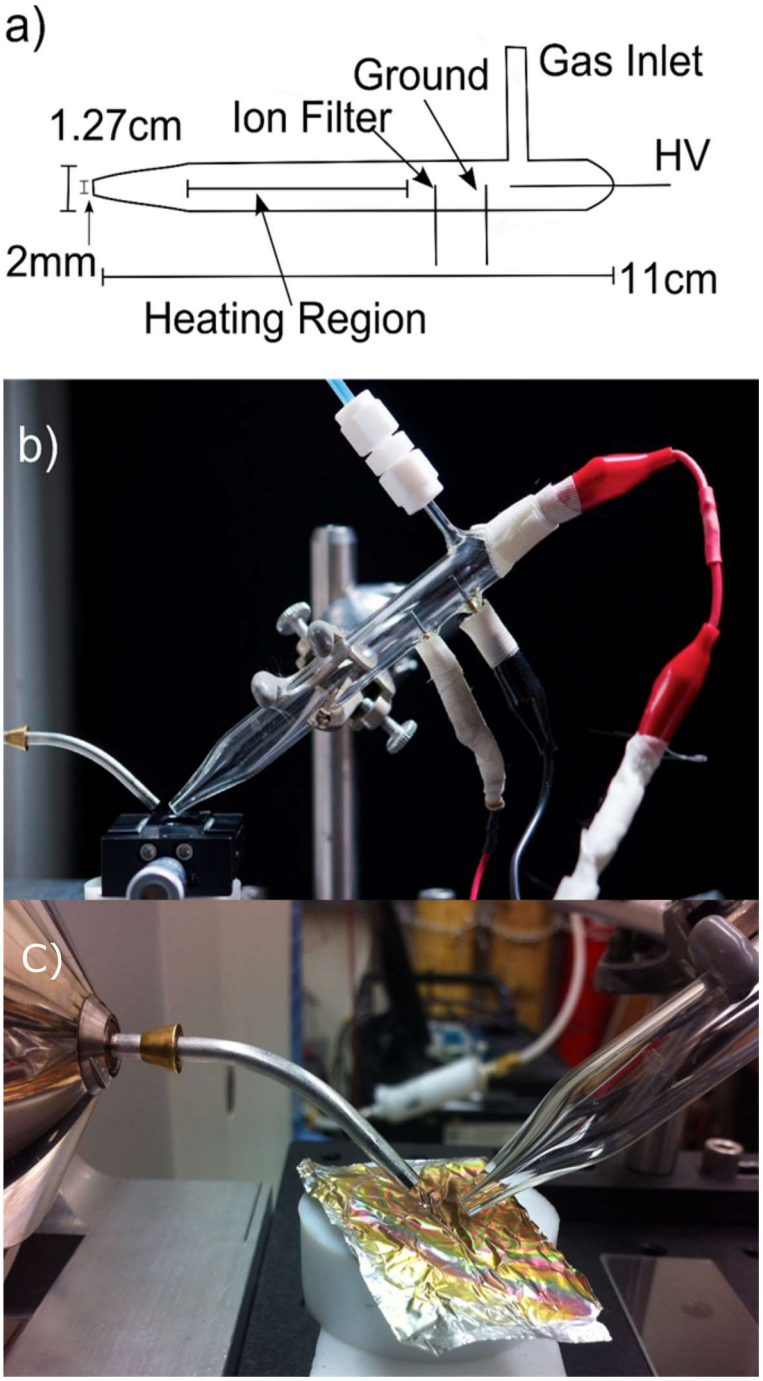

Figure 3.2. a) Schematic of the EZ-DART source, photographs of the b) EZ-DART source experimental setup and c) EZ-DART during sampling of THS aerosols. (Figure adapted from Upton et. al. 2017)

3.3.4 Sample Analysis by EZ-DART

In the study presented here, EZ-DART mass spectra of THS aerosols produced from the four gas mixtures and deposited on hv-Al foil were acquired at Caltech. To ensure sample preservation and reproducibility, the following systematic protocol was adopted: (1) DART mass spectra of a blank hv-Al substrate were acquired at the same temperature as the planned THS sample acquisition prior to each analysis; (2) The THS samples were removed from the freezer and analyzed with the EZ-DART within 5 minutes for room temperature spectra, and within 30 minutes for elevated temperatures. For elevated temperatures, spectra were accumulated while slowly increasing the heater temperature using manual temperature control (5-10°C/min with a maximum of 250°C), allowing for the monitoring of any temperature dependent changes in signal.

In order to limit the exposure of the samples and prioritize the identification of nitrogen containing compounds, only positive ion spectra were acquired. Analysis was performed at the location of highest deposition thickness, which corresponded to the position that was facing the center of the THS slit during deposition due to the planar nature of the expansion, and was approximately at the center of the sample. Since the EZ-DART samples a large area (2-5mm), ensuring a region of equal deposition for analysis was less relevant than ensuring sampling from a region of high deposition. The THS EZ-DART spectra were background subtracted, using the blank hv-Al foil spectra acquired before each sample, to allow for the analysis of lower intensity species. To allow for some structural analysis, collision induced dissociation (CID) was used to analyze the DART spectra. In CID, the parent molecules responsible for a specific mass peak in the spectrum are accelerated to a

high kinetic energy using an electric potential, at which point the excited parents collide with a buffer gas. This collision converts the kinetic energy to internal energy, which results in the breaking of hydrogen-bonded adducts or a covalent bond within the parent molecules and produces an MS/MS spectrum. The resultant spectrum therefore shows how the parent molecules fragment and allows for the identification of structural characteristics and the elucidation of multiple species within a single peak.[44] CID spectra were not background subtracted, leading to some contribution from background in the CID spectra. The CID spectra from the samples were compared with those from the hv-Al blank (shown in the supplemental information), after which only peaks showing major deviations from the blank in both intensity and mass were considered in subsequent analysis.

3.4 Results and Discussion

3.4.1 Comparing the DART spectra of the THS samples produced in four different gas mixtures

DART mass spectra were acquired for THS simulants produced in the following four gas mixtures: N_2-CH_4 (95-5), N_2-CH_4-C_2H_2 (91-5-4, acetylene), N_2-CH_4-C_6H_6 (90-5-5, benzene), N_2-CH_4-C_2H_2-C_6H_6 (86-5-4-5, acetylene and benzene). These spectra, shown in figure 3.3, were all background subtracted prior to analysis to eliminate complications from atmospheric contaminants.

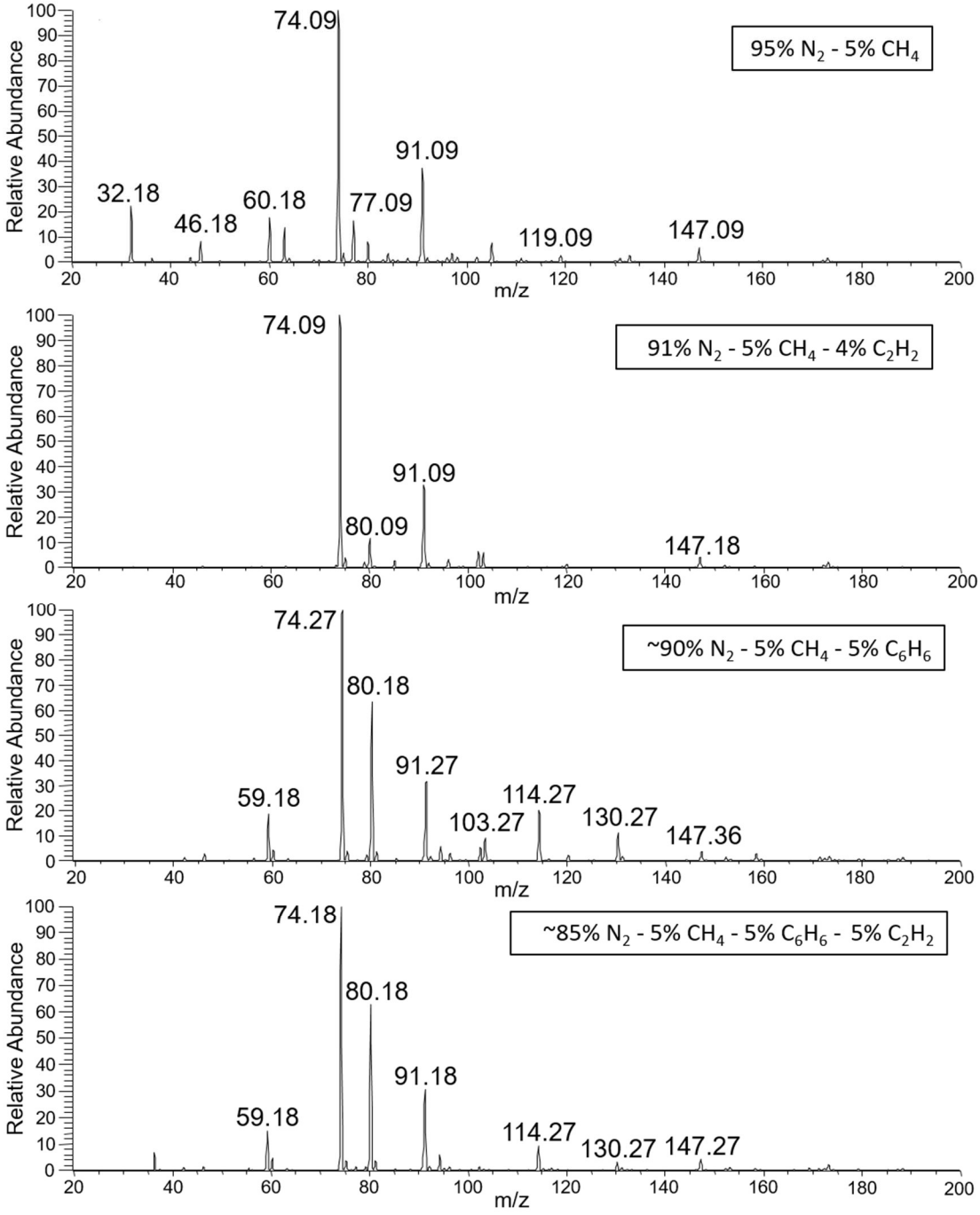

Figure 3.3. EZ-DART mass spectra of THS simulants collected at room temperature with ambient background subtracted. From top to bottom: 95-5 N_2-CH_4, 91-5-4 N_2-CH_4-C_2H_2 (acetylene), 90-5-5 N_2-CH_4-C_6H_6 (benzene), 86-5-4-5 N2-CH_4-C_2H_2-C_6H_6 (acetylene and benzene).

By comparing these four spectra, it is possible to determine the general effects of the different gas mixtures on the solid phase composition. The initial observation is the relative simplicity of all four spectra. Spectra were acquired up to 1000 m/z mass range, but their analysis was limited to the 20-200 m/z mass range due to the scarcity of peaks detected at higher masses. As seen in figure 3.3, the peak intensities drop off above 74 m/z. Furthermore, compared to DART mass spectra of other organic aerosols or petroleum, there are surprisingly few peaks in the THS sample mass spectra, even in the <200 m/z region. While competitive ionization effects may have contributed to this observation, complex spectra (more peaks and higher masses) have been observed in previous studies from samples with similar diversity, making the ionization effect a known minimal contributor. The discussion presented here regarding the types of molecules made in the THS experiment for each gas mixture is limited to the species predisposed to detection by DART-MS, i.e., with suitable volatility and proton affinity for DART ionization. This means that the DART analysis cannot be used to assess what the most abundant species overall are within the samples. On the other hand, by limiting the types of species detectable to high proton affinity compounds, the DART technique has the benefit of simplifying the analysis to mostly nitrogen containing compounds; the main goal of this study. Complementary mass spectrometry techniques will be used in the future to investigate the presence of less volatile and lower proton affinity species such as hydrocarbons.

Another advantage of DART is the ability to detect volatile species trapped within the sample during the experiment. The preservation of these compounds, especially those with high vapor pressures, is likely due to a matrix effect of the solid deposition. Since the solid grains are jet-deposited over long timescales (10-40 hours), it is likely that small volatile

molecules become trapped in the solid matrix that develops. This effect has already been observed on grains produced in COSmIC, where argon was trapped in the solid deposit and then evaporated, leaving holes in the deposit layers as seen by SEM. Furthermore, a recent IR study of the THS simulants has shown the disappearance of absorption features over time.[25] This effect could be explained by volatiles trapped within the solid slowly evaporating post deposition. Quickly freezing the samples and acquiring DART mass spectra directly after removal from the freezer, combined with this matrix effect, likely preserves these small volatile compounds and enables their subsequent detection. This matrix effect may also be representative of mechanisms occurring on Titan allowing for increased chemical diversity throughout the atmosphere. As aerosols accumulate in the atmosphere and settle into haze layers, a similar matrix effect could preserve small photochemically reactive organics. This may lead to the transport of more reactive species to the surface, in accumulated aerosol, allowing molecules not expected to be found on the surface to undergo chemistry outside of higher atmospheric layers.

Closer comparison of the DART mass spectra obtained with the four THS simulants shows more details about the effects of the different dopants on the composition of the solid phase. The most intense mass peaks (74, 80, 91 m/z) for all four mixtures are remarkably similar, suggesting that there are favored mechanistic pathways that produce these smaller, more volatile species. Major differences are observed as well. More species are detected for the 95-5 simulant in the <70 m/z mass range compared to the simulants produced in more complex mixtures, while new higher mass species (>91 m/z) are detected in the benzene doped simulants that are not present in the simulants produced in simpler mixtures.

The acetylene doped (91-5-4) simulant presents the simplest spectrum, which contains no major peaks in the <70 m/z mass range and fewer major peaks overall. This could imply that the chemistry induced by the presence of acetylene, a known precursor of benzene, in the gas mixture is mostly hydrocarbon based, and consequently not detectable with DART. The observed simplicity is also suggestive that nitrogen incorporation in this mixture is minimal, which is in agreement with the study in Part II, for which little nitrogen functionality was observed in the IR spectrum. The results of an unpublished x-ray absorption near edge structure (XANES) spectroscopy are also showing a much higher C/N ratio for N_2-CH_4-C_2H_2 mixture compared to N_2-CH_4 mixtures. From this comparison, it appears that acetylene has the most pronounced effect on the products detectable by DART, resulting in the decreased diversity of small polar molecules. This observation may have implications for nitrogen chemistry in Titan's atmosphere that will necessitate further investigation.

The spectra of the benzene doped (90-5-5) sample presents the same major mass peaks (74, 80, 91) as the 95-5 and acetylene doped (91-5-4) simulants, but shows an increase in the 80 m/z peak and the appearance of additional peaks. Therefore, the presence of benzene in the plasma discharge appears to lead to new synthetic pathways that are not occurring in other mixtures. One of the reasons could be that these reactions do not have time to occur during the short residence time of the gas within the active region of the plasma discharge in simpler mixtures where benzene needs to first be produced by chemical reactions. Comparison with the acetylene doped (91-5-4) sample shows that benzene and acetylene each have unique impacts on the chemistry.

For the simulant produced in the mixture with both dopants, acetylene and benzene, the mass spectrum appears to be a combination of the acetylene doped (91-5-4) and benzene doped (90-5-5) simulant spectra, as expected. The two benzene-containing simulants present very similar DART mass spectra, which is consistent with the IR analysis presented in Part II, where the IR spectra of the benzene containing mixtures were almost identical. The benzene chemistry dominates, since the quenching of additional peaks as seen in the acetylene doped (91-5-4) spectrum is not observed, whereas additional peaks from the benzene doped (90-5-5) are still observed with comparable relative intensity. All of these initial observations are suggestive of predicable mechanisms within the THS experiment, leading to quenching of complex chemistry and the resulting domination of smaller components.

3.4.2 Comparing the THS DART spectra acquired at room (17°C) and high (250°C) temperatures

Before further analysis is performed under the assumption that we are observing simpler products related to early and intermediate chemistry, some comparisons are necessary. We first compared the room temperature spectra of the four THS samples to those obtained with higher DART heater temperatures. From prior DART studies of complex organic mixtures, such as petroleum, it has been observed that increasing the temperature of the DART heater can result in the detection of low volatility species as well as species with higher masses. DART spectra were acquired while increasing the heater temperature for each of the four samples. Each sample but the benzene doped (90-5-5) displayed a signal

decrease consistent with the loss of volatile species. The DART spectra of the benzene doped simulant at room temperature and 250°C are shown in figure 3.4 for the low mass region.

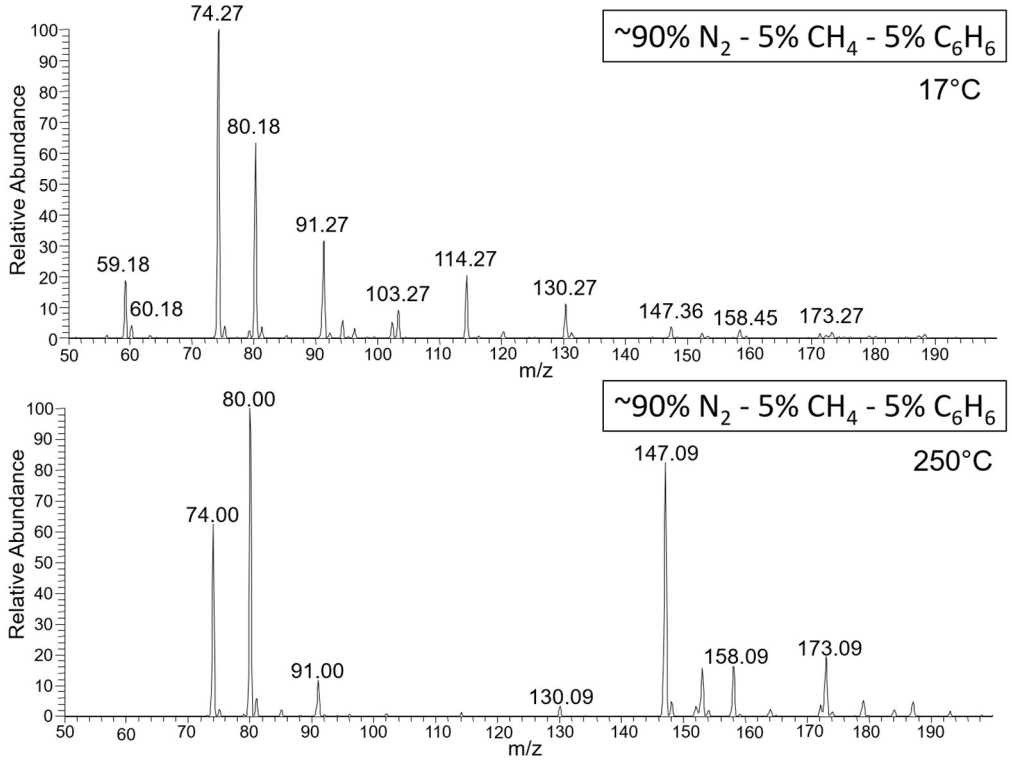

Figure 3.4. DART spectra of the N_2-CH_4-C_6H_6 (90-5-5) sample acquired at two different temperatures: Top: The same spectrum as reported in figure 3.3, collected at room temperature, Bottom: The spectrum collected at a recorded heater temperature of 250°C as measured at the EZ-DART heater.

The mass range of 50-200 m/z is shown since the high temperature spectrum was acquired with mass range of 50-1000m/z to enable the detection of any higher mass species. Since on a few lower intensity peaks were seen at masses >200m/z, a 50-200 m/z range is used for the comparison. The first observation to be made is the major difference between

the high temperature DART spectrum of the THS sample and those obtained with other complex organic samples: with the THS sample, an increase in the intensity of the low mass species was observed as opposed to the expected decrease. Furthermore, no new peaks appeared at elevated temperatures in the "gap" regions between the peaks detected in the low temperature spectrum, eliminating the possibility that low volatility-, DART detectable products exist within these regions. These two factors indicate that the products observed follow a predictable pattern biased towards the production of these lower molecular weight species. This supports the hypothesis that the pulsed plasma jet expansion configuration of the THS does not induce an over processing of the analytes, allowing for simpler chemistry to dominate the DART ionizable products.

The observation of products at higher DART heater temperatures for the benzene doped (90-5-5) sample fits with the results of the IR analysis performed in Part II, where the benzene containing samples showed large amounts of aromatic vibrational bands that could be due to polyaromatic hydrocarbons (PAH) polymers as the primary products. An abundance of low volatility polymers would facilitate the preservation of high volatility molecules. These molecules would be trapped in the lower volatility PAH polymers until the DART heater temperature was increased. This hypothesis does, however, call into question why high temperature spectra were not observed for the sample doped with both acetylene and benzene, since the benzene chemistry appears to dominate the DART detectable species. A reason for this difference may be lower production of these species, since the addition of acetylene appears to quench some of the chemistry seen in the 95-5 sample. Another factor may be lower production of the preservative PAH polymers for the 86-5-4-5 mixture. These effects could be confirmed with additional studies on mixtures with

various amount of acetylene and benzene dopants, which is beyond the scope of the present study.

The observation of aromatic features in the IR absorption spectrum of the benzene doped samples, and the observations of shifts in some band positions compared to the VIMS data acquired at Titan suggests the THS benzene doped samples are not representative of bulk Titan atmospheric chemistry. However, DART mass spectra obtained for the benzene doped samples could provide insight into the chemistry of a high benzene content microenvironment within Titan's atmosphere. Recently, analyses of CIRS data[45] has allowed the detection of benzene ice in Titan's atmosphere. The condensation of benzene could provide a benzene rich environment in which other atmospheric molecules could participate in aerosol-gas phase reactions, the products of which would not be observed in the bulk of Titan's atmosphere. Products from these local environments may provide a source of molecules not readily synthesized solely by the photochemistry of nitrogen and methane. Thus, the benzene doped samples provide insight into these benzene rich conditions, and possible implications for unique chemistry in Titan's atmosphere.

3.4.3 Comparing the DART spectra of a THS sample to a continuous plasma produced simulant

The second comparison we conducted consisted in looking at the differences between a THS simulant, which shows minimal over-processing as explained above, and a previously studied Titan aerosol simulant produced in a continuous plasma experimental setup, i.e., most likely over-processed. To this end, we chose to compare two aerosols produced from a 95%

nitrogen and 5% methane mixture: the 95-5 simulant produced in the pulsed plasma discharge of the THS setup and a simulant produced in a continuous plasma discharge by Smith et al. at the University of Arizona (apparatus details in He et al[16]). The Arizona simulant has been previously characterized in detail with multiple methods, including electrospray ionization ion cyclotron resonance mass spectrometry (ESI-ICR-MS). In that analysis, a large number of different compounds were found, making it a complex statistical mixture of carbon, hydrogen, and nitrogen.

With the comparison presented here, it is important to keep in mind that ionization by DART is a function of volatility and proton affinity. Since the THS DART mass spectrum was acquired at room temperature, the Arizona aerosol analogue was also tested at room temperature. A lower temperature decreases the likelihood of detecting heavier constituents, since only high volatility species are easily detected without heating. When the Arizona simulant was prepared for analysis a small amount of the powder was placed on hv-Al foil, adhered to the foil using 20 μL of anhydrous methanol, and allowed to dry. After this preparation, the analysis process was the same as for the THS aerosols. While using a solvent does not allow for the most direct comparison, it was required to keep the powder from being dispersed by the DART flow gas.

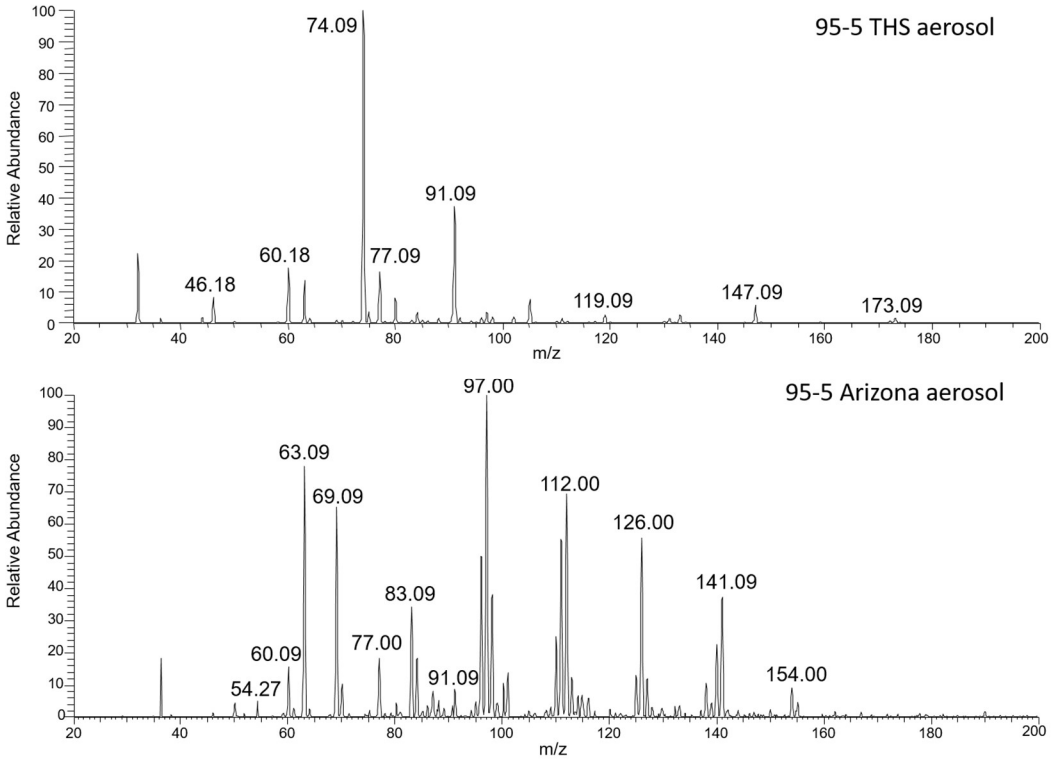

Figure 3.5. Room temperature DART spectra of the (Top) 95%N_2-5%CH_4 THS sample and a (Bottom) 95%N_2-5%CH_4 Titan aerosol simulant sample from the University of Arizona. Since the Arizona aerosol required solvation, a methanol trimer peak is visible at 97 m/z. Both spectra are background subtracted from ambient background.

The DART spectra of the Arizona simulant and the THS simulant acquired at room temperature are shown in figure 3.5. In the spectrum of the Arizona simulant, the base peak at 97 m/z is attributed to the methanol trimer, commonly seen in DART analyses of samples containing methanol. When comparing the two spectra, a difference in complexity between the THS and Arizona simulants is immediately visible: the Arizona simulant shows a greater number of peaks over the entire low mass region. Since ionization with DART is related to proton affinity, it can be assumed that the Arizona simulant contains more nitrogen-bearing compounds, leading to higher proton affinity. This increased nitrogen incorporation is likely

related to a more complex chemistry occurring in the continuous plasma discharge of the Arizona experimental setup. In the THS experiment, even though the high energy required to dissociate nitrogen is reached in the pulsed plasma discharge, there is only a short time (< 3μs) during which the nitrogen can react. In the Arizona experimental setup, in which the continuous plasma discharge allows for the continuous dissociation of both nitrogen gas and products over the course of the experiment, resulting in significantly more processing of the Arizona simulant compared to the THS simulant, and the subsequent incorporation of more nitrogen-containing molecules in the Arizona solid aerosols. The higher number of peaks observed in the Arizona sample DART spectrum supports this assessment and the initial hypothesis that the THS experiment allows for the observation of early and intermediate chemical products. The simplicity of the THS simulant DART spectra has allowed a more in depth structural analysis, the results of which are presented below with possible mechanisms for their creation in Titan's atmosphere either reported from prior work or proposed.

3.4.4 Analysis of peaks observed in the THS DART spectra

While the THS DART mass spectra from all four mixtures (figure 3.3) show relatively few peaks, the non-exact mass resolution of the ion trap mass spectrometer used, combined with the propensity of DART ionization to form adducts with both water and ammonia, complicated the analysis. To allow for some structural analysis, collision induced dissociation (CID) was used. As discussed above CID allows for the structural identification through fragmentation. By identifying adducts and fragments ions, molecular formulae

could be suggested. Formulae and compounds reported from this data analysis were assigned using possible combinations of carbon, hydrogen, and nitrogen, giving higher consideration to possible structures that could account for losses observed in CID and adduct formation when applicable. Since polar samples have been observed to readily adduct to water and ammonia in prior studies,[46] only polar compounds were assigned as adducts. In addition to adducts and protonated ions, the detection of molecular ions was also considered during the analysis.

CID analysis of all species was not attempted in this work. Only m/z values for which CID spectra were consistent for multiple scans were considered. Since some of these peaks were also concurrent with background, only the ones showing at least an order of magnitude difference in signal intensity with background CID spectra were analyzed (as shown in the supplemental information or SI). Additional CID data recorded but not analyzed in this work are reported in the SI for possible future analysis, pending new insights. Since CID targets a species based on m/z and an isolation width of 2 m/z was chosen (ensure capture of less stable species), the resultant MS/MS can be more complex than expected. High resolution mass spectrometry analysis of a Titan aerosol simulant similar to the Arizona aerosol showed that even a single nominal mass could contain multiple peaks, each with their own possible structural isomers. Although the THS simulant is simpler than the Arizona aerosol, there is still the high probability for multiple species within a single nominal mass and isolation width. As such, the CID spectra shown below are a combination of fragments from each compound within the isolation width. Taking this into consideration, not all fragments in each result CID spectra were identified or discussed in this work. Any compound identifications were made based on readily interpretable fragments with the understanding

that contribution from other species was unavoidable. Before going into the details of the CID analysis, we first focus on peaks for which no CID data was obtained but assignments could be made.

3.4.4.1 Peaks at 80 m/z and 32 m/z – no CID

No CID fragmentation products were recorded for the 80 m/z peak. This peak is visible in the 95-5 DART spectrum, but undergoes a slight increase in intensity in the acetylene doped (91-5-4) DART spectrum, and is significantly more intense in the benzene doped (90-5-5) and acetylene and benzene doped (86-5-4-5) DART spectra. This 80 m/z peak could be related to the 79 m/z ion peak observed in the gas phase analysis (see Part 1). The peak at 79 m/z was only observed in the benzene doped (90-5-5) and acetylene and benzene doped (86-5-4-5) samples in the gas phase, which is in agreement with the substantial increase in 80 m/z peak intensity observed in the DART data for those two mixtures. The CID data for the benzene doped (90-5-5) sample, reported in the SI, shows a reaction product of 96 m/z, relating to a reaction with water in the ion trap. CID spectra for the other three mixtures were too low in intensity to be analyzed, which is expected due to their lower intensity compared to the benzene doped (90-5-5) sample.

Because both 79 and 80 m/z were observed in Part 1, the formulae presented in that work were used as the starting point here. While molecular ions are observed with DART, protonated species are more common, so only formulae for 79 Da were considered. Out of the two formulae proposed in that work, pyridine stood out as it has been observed in other Titan aerosol analogues.[29, 47] Because a reaction product was observed at 96 m/z in CID,

neat pyridine was also tested with DART to verify if a similar reaction would occur. 80 m/z was observed in the overall DART spectrum for pyridine and 96 m/z was observed in the CID spectrum (shown in the SI), making pyridine the most likely assignment for the 80 m/z peak.

If we consider that pyridine is the molecule observed in all four samples at 80 m/z, a mechanism needs to be proposed to not only explain its synthesis in each condition, but also provide insight into the intensity differences observed between the four samples. The intensity comparison does enable a starting point from which a mechanism can be suggested. The low intensity of the 80 m/z peak in the acetylene doped (91-5-4) sample suggests that acetylene does not play the largest role in the production of pyridine, but still allows for the production of a small amount. Mechanisms for the production of pyridine in Titan's atmosphere typically involve products made from acetylene. When considering the production of pyridine, Wilson and Atreya, 2003 cite that the typically expected mechanism of $C_5H_6 + N \rightarrow C_5H_5N + NH$, which is exothermic by 95 kJ/mol, would be unlikely on Titan due to the large energy barrier for the creation of C_5H_6 and thus cite the $C_4H_5 + HCN \rightarrow C_5H_5N+H$, endothermic by -122 kJ/mol, as a possible minor pathway by which pyridine could be produced.[48] This being a minor pathway is supported by the relatively small production of pyridine in the acetylene-doped (91-5-4) and 95-5 samples.

The inclusion of benzene though appears to be key for the larger relative production of pyridine, considering the substantial increase in the relative intensity of pyridine for mixtures with benzene. The direct substitution of nitrogen into benzene within the higher energy plasma needs to be ruled out as a reactionary route for pyridine production with a benzene dopant. Zhang and associates studied the different products of benzene with various

plasmas.[49] In that study, they found that pure nitrogen did not allow for the production of large amount of pyridine, air provided slightly more, and a 1% NO in nitrogen produced the most pyridine. They thus invoked the production of NO radicals in their mechanism for the production of pyridine by direct substitution. As the THS experiment uses UHP nitrogen and methane, NO will not have a mechanistic side effect on the production of pyridine and a different mechanism needs to be invoked. Parker and associates studied different mechanistic pathways for pyridine in an experiment at the Advanced Light Source using vinyl cyanide and phenyl radicals produced by pyrolysis.[50] The production of C_4H_6, proposed as a reactant for the production of pyridine and a possible product from benzene, was not observed in their experiment. This leads to the recombination of vinyl cyanide with either vinyl radical or cyanovinyl radical as the most likely pathways. A computational comparison found that reaction between vinyl cyanide and cyanovinyl radical had no entry barrier, which would allow this reaction to proceed at cold temperatures. Additionally, phenyl radical was cited as the progenitor of cyanovinyl radical through hydrogen abstraction, and the observation of aromatic vibrational modes in the IR analysis of the THS solid samples (Part II) suggests phenyl radical is indeed produced. This mechanism, along with the minor pathway described above, provide evidence for the differing amounts of pyridine production between the four THS samples. The recent observation of vinyl cyanide on Titan 51 and the prior observation of benzene[52, 53] suggest that investigation of this mechanism could be relevant for the production of pyridine on Titan.

Another peak for which CID results were not obtained was 32 m/z observed only for the 95-5 sample. Because this peak was observed in extremely low abundance in the background DART spectrum (as reported in the SI), it can be assumed that it is not due to

the presence O_2^+ produced by the EZ-DART source. The only other possibility is methylamine, which can be produced from the recombination of the amino and methyl radicals. Amine IR bands have been reported in Part II for each of the four THS samples, so the observation of the simplest amine is reasonable. The observation of 46 m/z in the 95-5 sample suggests the presence of ethylamine or its isomers, which follows from the production of methylamine with the inclusion of another methyl radical. Production of propylamine, or an isomer, would follow sequentially, and is seen at 60 m/z. These products are expected to be produced in Titan's atmosphere, so their observation is not unprecedented. While CID of these species would be helpful for exact identification, they were too low in mass or intensity to provide spectra in the study presented here. The ease of synthesis for these molecules, combined with the observations of amines in the IR analysis (Part II), make the assignments of these peaks as simple amines the most reasonable conclusion.

As discussed above, the preservation of gaseous and high volatility species has already been observed in prior works using the COSmIC chamber, where argon was trapped in the solid matrix and later released after sample collection. Since the THS samples used in the present study were quickly stored below the boiling temperature of methylamine and ethylamine, their preservation until DART analysis would be considered feasible. The observation of these amines in only the 95-5 sample may be related to a variety of factors, the most likely of which is that benzene and acetylene produce radicals that combine with the methyl or amino radicals from the nitrogen and methane producing different products, some of which not ionizable with DART. The observation of these simple amines in the 95-5 sample, produced in the simplest gas mixture, suggests that the THS experiment can be used to simulate the early stage of Titan's chemistry.

3.4.4.2 74 m/z CID analysis

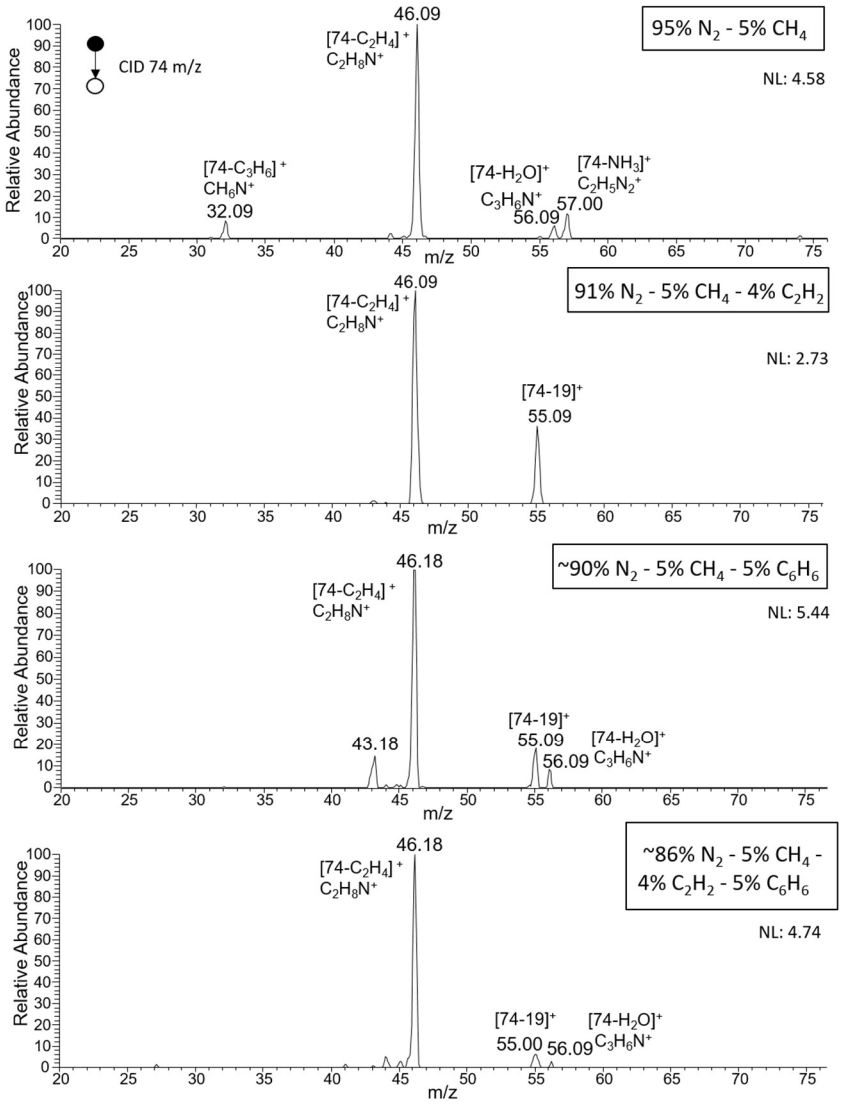

Figure 3.6. CID spectra of the 74 m/z DART peak for each sample, from top to bottom: 95-5 N_2-CH_4, 91-5-4 N_2-CH_4-C_2H2 (acetylene), 90-5-5 N_2-CH_4-C_6H_6 (benzene), 86-5-4-5 N_2-CH_4-C_2H_2-C_6H_6 (acetylene and benzene). Major fragments and losses are labeled. Overall intensity is reported for each spectrum as the normalized target level (NL).

74 m/z is the base peak in the DART mass spectrum for all four samples and was therefore the first target for analysis by CID. The CID spectra for 74 m/z are shown in figure

4.6, displaying the complexity contained within a single peak. Note that the peak at 74 m/z is one of the first peaks for which higher complexity would be expected due to an increased number of possible isomers. Since more isomers are possible within the 74 m/z peak, identifications were made with caution. Conclusions were drawn from the trends between observed species where an exact identification could not be made. Even though 74 m/z is the base peak for each sample, the peaks present in the CID spectra had very low intensity, suggesting the presence of several parent molecules including adducts and isomers at that mass. It is important to note that the CID data enable us to study some of the isomers, but do not always allow for complete characterization of each species within the analyzed peak.

In the CID spectra of the 74 m/z peak, the major product peak observed in all four samples is 46 m/z. Because it results from the loss of 28 Da (C_2H_4 – ethylene) from the parent molecule, this product is most likely ethylamine (protonated in the CID spectrum: $C_2H_8N^+$). For the ethylamine product to consistently be present in the spectra despite their low intensity, it is assumed that multiple routes must be available for the species at 74 m/z to lose 28 Da. Comparison to other MS/MS spectra 54 has led to the assignment of diethylamine for the 74 m/z species that results in the 46 m/z CID product. Additionally the structure of the diethylamine molecules allows for the loss of C_2H_4 from either side, explaining why this product is consistently present even in low intensity spectra. The synthesis of diethylamine likely follows from other smaller amines, with the addition of two methyl radicals directly to the amine. The 46 m/z CID product is the only one that is common to all four THS samples. This demonstrates that even the most abundant mass peak results from the presence of different parent molecules being synthesized in each sample.

In the 95-5 CID spectrum, the 57 and 56 m/z products are adducts with ammonia and water respectively. While the 57 m/z product could be proposed as an amine loss from 74 m/z itself, as opposed to an adduct, that is unlikely for multiple reasons. The most obvious reason is that no peak was observed at 57 m/z in the overall DART spectrum. The loss of 17 Da has been observed from primary amines in prior work involving the EZ-DART 41, but in those cases the loss product was also detected in the overall spectrum. This is not the case for the background subtracted 95-5 DART spectrum presented here (figure 3.3). Also, the most likely compound for which an amine loss would be observed would be methylguanidine, but in that case other CID products would be expected for that species, such as 43 m/z, which is not detected in the 95-5 CID spectrum. For these reasons, we assign the 57 m/z product as being from an ammonia adduct, with the most likely formula being $C_2H_4N_2$ (protonated in the CID spectrum: $C_2H_5N_2^+$), for which aminoacetonitrile and methyl cyanamide are the two stable structural isomers. Other isomers would contain azides, radicals, or permanent charges, all of which would not be expected to form adducts. Because methyl cyanamide would undergo spontaneous trimerization above its melting point, we assign aminoacetonitrile to the 57 m/z species. Aminoacetonitrile has been detected in other Titan simulants as well as in the interstellar medium,[55] and its synthesis from methyl, amino, and cyano radicals is possible in Titan's atmosphere.

The 56 m/z peak in the 95-5 CID spectrum is due to a loss of 18 Da and is identified as a water adduct, commonly observed in DART analysis. The most likely formula for this species would be C_3H_5N (protonated in the CID spectrum: $C_3H_6N^+$), for which two of the most stable isomers are propionitrile and propargylamine. Since both of these products are stable and able to adduct with water, it is difficult to assign 56 m/z to one isomer over another.

Consequently, it is necessary to make comparisons to other analyses to attempt an assignment. Comparison with the IR data reported in Part II suggests a propionitrile identification, since propargylamine contains a terminal alkyne and the corresponding vibration was not observed in the IR spectrum for the 95-5 sample. Additionally, observation of propargylamine would also be expected in the acetylene doped (91-5-4) sample due to the presence of the terminal alkyne, but no 56 m/z product peak is present in the 74 m/z CID spectrum for that mixture. These factors led us to tentatively assign propionitrile to the 56 m/z product ion in the 95-5 sample. The 74 m/z CID spectra for the two benzene doped (90-5-5 and 86-5-4-5) samples also show a peak at 56 m/z, but it is much more difficult to identify. The IR analysis described in Part II reported bands associated with terminal alkynes and amines, in addition to bands for possible nitriles. Due to this discrepancy, the 56 m/z peak cannot be assigned for the benzene doped samples, but likely corresponds to one of the two isomers proposed for the 95-5 sample.

The 32 m/z peak in the 95-5 CID spectrum is the simplest to assign since the 32 m/z mass peak is also observed in the overall DART spectrum and has already been identified as methylamine. In the 74 m/z CID spectrum, this peak is produced from the loss of 42 Da (C_3H_6) from 74 m/z. The 74 m/z species generating this product ion is identified as N-methylpropylamine, with the 42 Da loss corresponding to the loss of the propane from the compound. The presence of this isomer, combined with the low overall intensity of this spectrum, shows that multiple isomers should be expected for any peak analyzed with DART.

The observation of a peak at 43 m/z in the benzene doped (90-5-5) sample is more difficult to assign since it is indicative of a 31 Da loss, possibly methylamine. The 43 m/z

peak in this spectrum must have higher proton affinity to retain the ionization over the methylamine, eliminating the possibility of it coming from N-methylpropylamine as assigned in the 95-5 DART spectrum. Taking that into account, the most likely formula for the 43 m/z fragment would be CH_2N_2 (protonated in the CID spectrum: $CH_3N_2^+$), making the original parent formula $C_2H_7N_3$. This would place the most likely identification as methylguanidine for which 43 m/z is an expected fragment. The lack of other fragments expected in the methylguanidine CID spectrum however, makes this identification tentative, and will require additional analysis in the future to confirm.

A product peak at 55 m/z is observed in all CID spectra except for the 95-5 sample. This peak corresponds to a loss of 19 Da and is therefore difficult to assign. It cannot be identified as a water loss from a 73 m/z peak contained in the CID isolation width since there is no 73 m/z peak observed in the overall DART spectrum (not even without background subtraction). This leaves the product as the likely result of a two-step loss process, thus too difficult to identify with the data available, and requiring further analysis in the future.

In summary, with the data obtained through CID analysis of the 74 m/z peak, we can positively identify diethylamine, aminoacetonitrile, propionitrile, and N-methylpropylamine as compounds contained in the 74 m/z peak. The diversity of compounds shows how necessary CID analysis is for the identification of species in these simulants. The synthesis of these species all fit well within mechanisms discussed in earlier works, even though amines have yet to be identified on Titan. The observation of these and other amines in the overall data show the preservation of small molecules over the course of accumulation and analysis. This suggests that these amines could be produced on Titan and be available for synthesis of other products.

3.4.4.3 91 m/z CID analysis

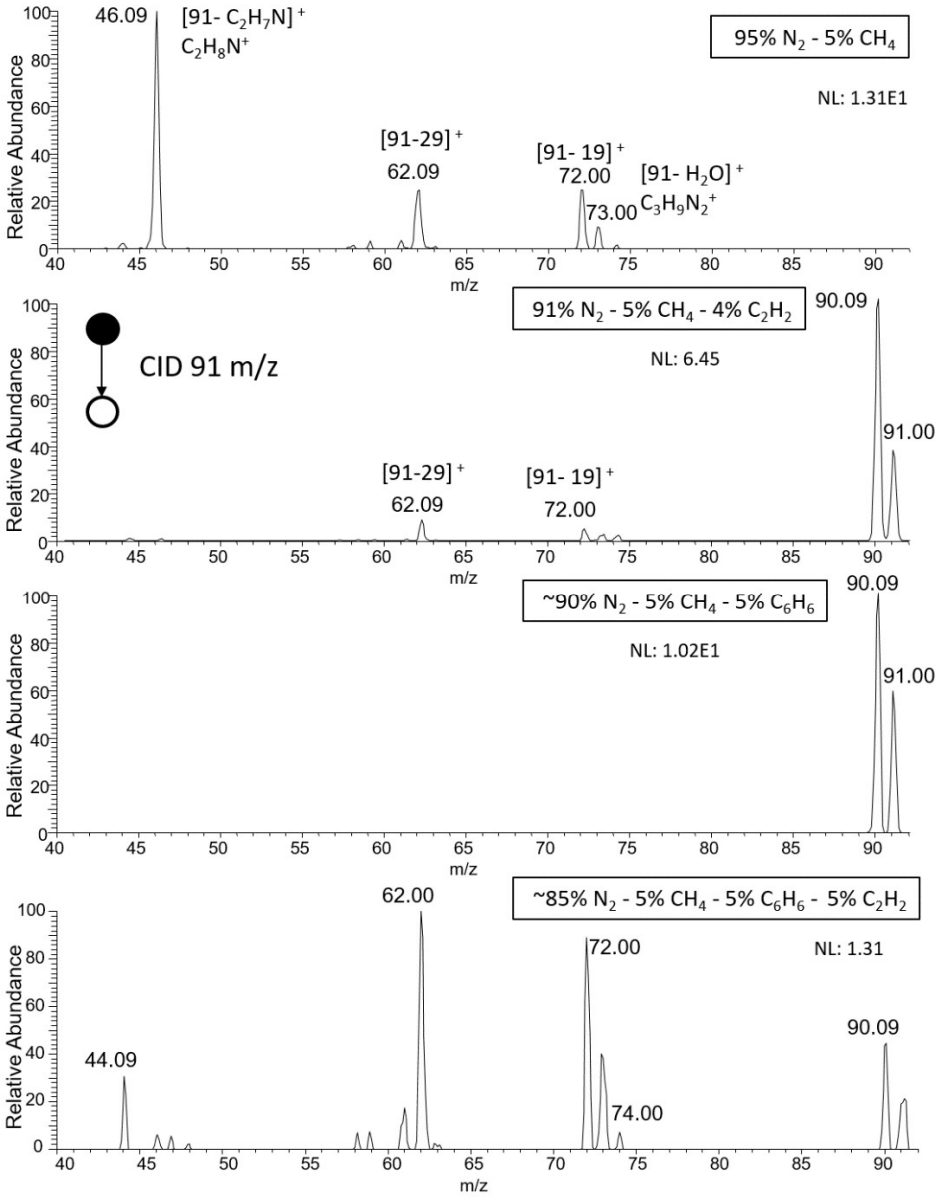

Figure 3.7. CID spectra of the 91 m/z DART peak for each sample, from top to bottom: 95-5 N_2-CH_4, 91-5-4 N_2-CH_4-C_2H_2 (acetylene), 90-5-5 N_2-CH_4-C_6H_6 (benzene), 86-5-4-5 N_2-CH_4-C_2H_2-C_6H_6 (acetylene and benzene). Major fragments and losses are labeled. Overall intensity is reported for each spectrum as the normalized target level (NL). The 86-5-4-5 spectrum is unlabled due to extremely low overall intensity.

Since 91 m/z was the next most intense peak common between all four samples, it was also analyzed with CID. The resulting CID spectra for all four samples are shown in figure 3.7. It should be noted that the CID spectrum of the acetylene and benzene doped (86-5-4-5) sample was very low in intensity and was not extensively analyzed in this work. However, because all peaks in that spectrum were an order of magnitude higher than the background CID, they were still used for comparison. Initial inspection of the four different spectra shows how much impact the inclusion of a dopant can have on the synthesis of different compounds within the THS. The THS chemistry appears to be more diverse in the acetylene and benzene doped (86-5-4-5) sample, with the detection of a broader range of fragments in the CID spectrum. This diversity could also account for the lower intensity of the CID spectrum for this sample, since having many different products contained within one peak would decrease the overall intensity of the CID spectrum. In the CID spectrum of the 95-5 sample, the base peak is at 46 m/z. This 46 m/z product is easily explained as a dimer, since 46 m/z is also observed in the overall DART spectrum for the 95-5 sample, and has been identified in that case as ethylamine. Seeing a dimer for ethylamine is reasonable, considering there is also evidence of a dimer for methylamine at 63 m/z in the overall spectrum for the same sample.

In the 91 m/z CID spectra for the acetylene doped (91-5-4) and benzene doped (90-5-5) samples, the major peaks are 90 and 91 m/z, which suggest the presence of a molecular cation or extremely stable protonated species which does not readily undergo fragmentation, and only loses a single hydrogen when fragmentation does occur. The production of this compound seems to be heavily influenced by the presence of benzene, considering the

benzene sample contains no other fragment ions. The observation of 90 m/z is unlikely to be from the isolation width used (i.e. coming from a 90 m/z peak in the DART spectrum), since there is no 90 m/z peak observed in the overall DART mass spectra. This suggests that 91 m/z is a molecular cation, which would be more likely observed for a species with some type of aromaticity or conjugation. The two most probable formulae for 91 m/z are $C_7H_7^+$ and $C_6H_5N^+$. For $C_7H_7^+$, the only likely compounds would be benzyl cation or tropylium cation. Observation of either of these species by DART would be unlikely since both would be produced from the ionization of toluene, which was not detected by EZ-DART when tested as a reference. This compound thus likely contains a ring structure with the formula of C_6H_5N, for which there are several possible isomers, the most stable of which would be ethynylpyrrole or cyclopentadienecarbonitrile. Neither of these are fully conjugated, but they could reasonably be produced in the benzene or acetylene doped mixtures, since amines and nitriles were detected in the IR data for both of these dopants. While the production of either is questionable considering the lack of fragments, an explanation may exist in the ionization process. Indeed, a lack of fragments was also observed for the protonated pyridine observed at 80 m/z in the overall DART spectrum. Because of its similarity with pyridine, in that regard, ethynylpyrrole seems to be a more likely possibility. The synthesis of pyridine was proposed as reasonable due to the inclusion of benzene. It is possible that phenyl radical could also assist in the production of other nitrogen containing rings.

The 73 m/z peak present in the CID spectra of both the 95-5 and acetylene doped (91-5-4) samples is due to a loss of 18 Da, and is thus identified as a water adduct. This product is most likely $C_3H_8N_2$ (protonated in the CID spectrum: $C_3H_9N_2^+$), since $C_4H_{10}N$ does not contain any isomers without a permanent charge. Attempting to assign the $C_3H_8N_2$

is difficult though since there are many possible structural isomers, but comparisons with other analytical data can assist in the characterization. From the IR analysis in Part II, we know that imines have been observed for the 95-5 sample and that no bands corresponding to an N-N bond were reported. A three or four member ring would be unlikely due to the steric strain, leaving possible candidates as an imine, five membered ring with two nitrogen atoms, or an alkene with two amines. A full identification cannot be completed without more data such as subsequent CID, which was not conducted in the present study. Imines and amines are good candidates though since they would be in agreement with both the THS IR analysis and other Titan aerosol simulations and models.

The 72 m/z fragmentation peak observed in both the 95-5 and acetylene-doped samples is from a loss of 19 Da, which is not from a single process and thus not identifiable with the data presented here, similar to the 55 m/z peak from the CID of 74 m/z. The 62 m/z fragment peak detected in both the 95-5 and acetylene doped (91-5-4) samples, corresponds to the loss of 29 Da, which can be assigned to the loss of methylimine, considering imines have been proposed to exist on Titan and also reported in earlier work.[25, 56, 57] After this point, assignment becomes much more difficult, since the 62 m/z fragment does not match expected possible products that, when combined with a methylimine loss, allow for a stable parent compound. This is not a 28 Da loss from 90 m/z since 90 m/z is not observed in the overall unsubtracted mass spectrum and 62 m/z is not seen in the background CID, indicating that it must come from the sample. It is possible that this is another two-step process. The data presented here cannot differentiate between a methylimine loss and a two-step process, but the latter seems to be a more reasonable explanation since two-step process peaks are also seen in the low intensity CID spectra of 74 m/z.

In summary, the CID spectra of the 91 m/z peak are more difficult to analyze and have only led to the identification of an ethylamine dimer, tentatively ethynylpyrrole and an imine or amine with a formula of C3H8N2. The stark contrast seen between the 95-5 sample and the more complex samples indicates that the inclusion of the dopants can not only induce the production of more complex species that cannot be produced with only nitrogen and methane in the truncated chemistry of the THS, but can also suppress the production of certain compounds.

3.4.4.4 114 m/z CID analysis

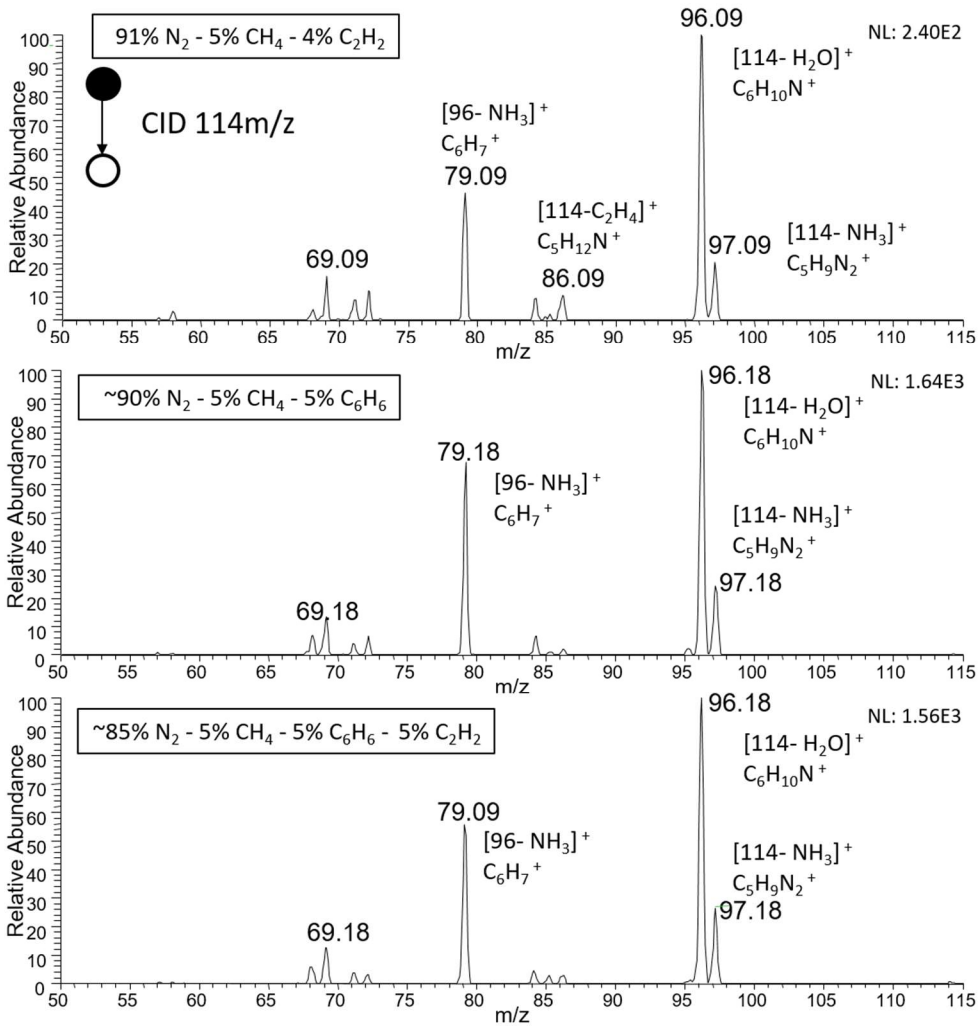

Figure 3.8. CID spectra of the 114 m/z DART peak for the three complex samples, from top to bottom: 91-5-4 N_2-CH_4-C_2H_2 (acetylene), 90-5-5 N_2-CH_4-C_6H_6 (benzene), 86-5-4-5 N_2-CH_4-C_2H_2-C_6H_6 (acetylene and benzene). Major fragments and losses are labeled. Overall intensity is reported for each spectrum as the normalized target level (NL).

The 114 m/z peak appears only in the DART spectra of the doped samples. The intensity of the 114 m/z peak is extremely small in the acetylene doped (91-5-4) sample but still present. In the benzene doped (90-5-5 and 86-5-4-5) samples however, the intensity of

the 114 m/z is much higher. In the resultant CID spectra, the first major fragment ion for all three samples is at 96 m/z and corresponds to a loss of 18 Da from the parent ion, therefore identified as a water adduct. The second most intense CID peak, at 79 m/z, is difficult to explain as a fragment from 114, since 35 Da does not add up to a possible fragment by itself, and 35 Da is higher than what we would expect for a two-step process.

In the benzene doped (90-5-5) and acetylene-and-benzene-doped (86-5-4-5) cases the peak intensity for the CID 96 m/z fragment ion was high enough to perform another CID step, shown in figure 3.9. In these MS^3 spectra, 79 m/z appears as a fragment of 96 m/z, indicating that the 79 m/z peak is from two concurrent losses: the loss of the adducted water, followed by a loss of 17 Da an amine from the 96 m/z species. A doubly adducted species, allowing for the loss of both water and ammonia adducts, has never been reported in prior DART studies, indicating that this is an amine loss, not the loss of an ammonia adduct. Previous work with the EZ-DART[41] has shown that primary amines are readily lost with DART sampling, supporting the identification of 79 m/z in the MS/MS spectrum as the loss of a primary amine from 96 m/z. In the case of the 114 m/z CID, the first CID scan could easily have broken the adduct species and also caused the loss of a primary amine, which would explain the 79 m/z peak. In addition, the other major peak at 68 m/z in the MS^3 scan is due to a loss of 28 Da, which could correspond to a loss of CH_2N or C_2H_4. By comparing these losses to other CID spectra of compounds with relevant chemical formulae, we can assign aminopyrimidine to the 96 m/z CID product. This compound would account for the loss of the primary amine, since other similar pyrimidine compounds produce an M-H+ fragment ion, matching the observation of 79 m/z. While other compounds are also possible for these spectra, aminopyrimidine accounts for the two major fragments. Moreover, the

presence of a very small amount of 96 m/z in the overall DART mass spectra provides further support for this assignment. Identification of the 97 m/z peak was not attempted due to MS^3 spectra being obtained from that mass. The other peaks in the CID spectra likely correspond to additional isomers from the 114 m/z and were not examined in detail due to their low abundance compared to the aminopyrimidine peaks.

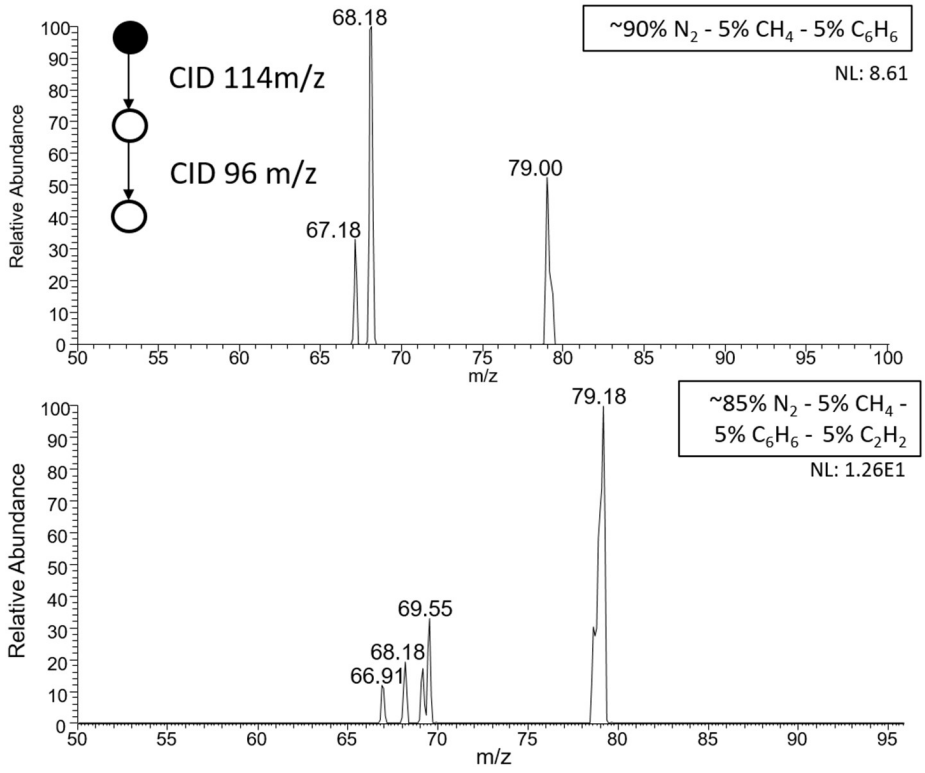

Figure 3.9. MS^3 spectrum of 114 m/z - 79 m/z for the two benzene doped samples, from top to bottom: 90-5-5 N_2-CH_4-C_6H_6 (benzene), 86-5-4-5 N_2-CH_4-C_2H_2-C_6H_6 (acetylene and benzene). Overall intensity is reported for each spectrum as the normalized target level (NL).

The finding of a pyrimidine-type molecule in these samples is of great interest for its prebiotic relevance since pyrimidine is a precursor of nucleobases. The production of

aminopyrimidine seems to be enhanced when benzene is present, and therefore it is likely that the synthesis of aminopyrimidine involves a mechanism comparable to that of pyridine, where acetylene can be used for the synthesis but phenyl radical can assist at low temperatures. At high temperature, a mechanism involving hydrogen cyanide and acetylene radical cation is known to produce a pyrimidine cation.[58] In the low-temperature processes of the THS experiment however, no pyrimidine production was observed in the acetylene doped only sample. Consequently, that mechanism is likely not the one responsible for the production of the aminopyrimidine observed in the THS samples. Taking that into consideration, it is likely that phenyl radical provides assistance to the synthesis, similarly to the pyridine production process. Comparing the intensities of the 79 m/z peak in the MS^3 spectra for the benzene doped (90-5-5) and the acetylene and benzene doped (86-5-4-5) samples suggests that aminopyrimidine production is enhanced when both dopants are included. From this perspective, it is possible that both acetylene and hydrogen cyanide are included in the synthesis of aminopyrimidine, but phenyl radical enhances the synthesis at the low temperatures used in the pulsed plasma discharge. This suggests that pyrimidine could be produced on Titan in benzene rich areas, since both hydrogen cyanide and acetylene would be readily available. Considering that the possibility of nucleic bases produced from acetylene on Titan has been discussed in prior work,[59] the observation of aminopyrimidine from the benzene doped samples shows the interest of investigating the benzene Titan chemistry further in future experiments.

3.4.4.5 119 m/z CID analysis

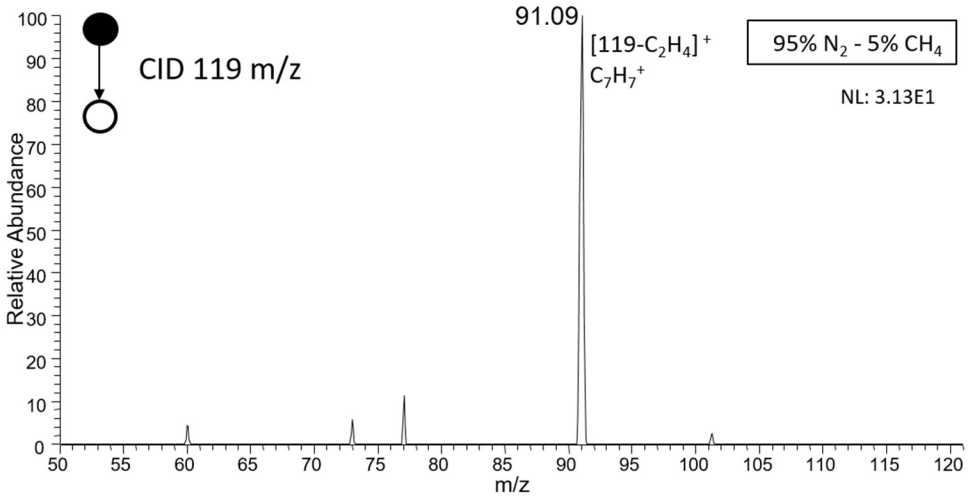

Figure 3.10. CID spectrum of the 119 m/z DART peak for the 95-5 N_2-CH sample. Overall intensity is reported as the normalized target level (NL).

The 119 m/z peak is only observed in the 95-5 sample. The CID analysis of that peak revealed that this compound shows no adduct formation, and only produces a major fragment of 91 m/z from a loss of 28 Da, i.e., either CH_2N or C_2H_4, both of which are possible for this sample considering that imines have been detected in the IR analysis. The high intensity of the 91 m/z peak implies it is a stable fragment produced from a favored fragmentation pathway, suggesting it could be due to a tropylium cation from a toluene-like parent ion. This would imply that the 91 m/z fragment results from a loss of 27 Da only, which would correspond to a hydrogen cyanide (HCN) loss. Such a loss would also be reasonable considering the presence of cyanides in this sample, but the resulting formulae of C_8H_8N for the parent molecule does not produce any viable chemical structure. As a consequence,

C_9H_{10} seems the most likely formula, and methylstyrene the best assignment since it accounts for the observation of a 91 m/z CID fragment resulting from an ethylene loss.

While the observation of hydrocarbons is known to be difficult in DART, α-methylstyrene has been observed before at high temperature,[60] indicating that some assistive ionization processes may be occurring in this sample. This assignment would also account for the lack of adduct formation, which is usually extremely common for DART detectable species. The production of methylstyrene could be questioned as coming from the background, but since this peak was not seen in any other sample and is observable even with background subtraction, that is unlikely. Observation of this compound in only the 95-5 sample is curious, since both benzene and acetylene should contribute to its production. A likely possibility is that the benzene and acetylene are consumed in other processes which prohibit the production of a small aromatic such as methylstyrene. Modeling could provide insight into why this product is only seen for the 95-5 sample and not the others. This could lead to interesting implications for Titan chemistry.

As the molecular mass increases, the exact identification of species via one-step CID becomes difficult due to the increasing number of structural isomers possible. As a consequence, the following CID analyses on higher mass peaks was conducted with a focus on identifying losses and chemical formulae with the most stable and reasonable isomers. Any compound suggestions will need to be studied with higher mass resolution or other methods in the future to identify possible species with increased confidence.

3.4.4.6 130 m/z CID analysis

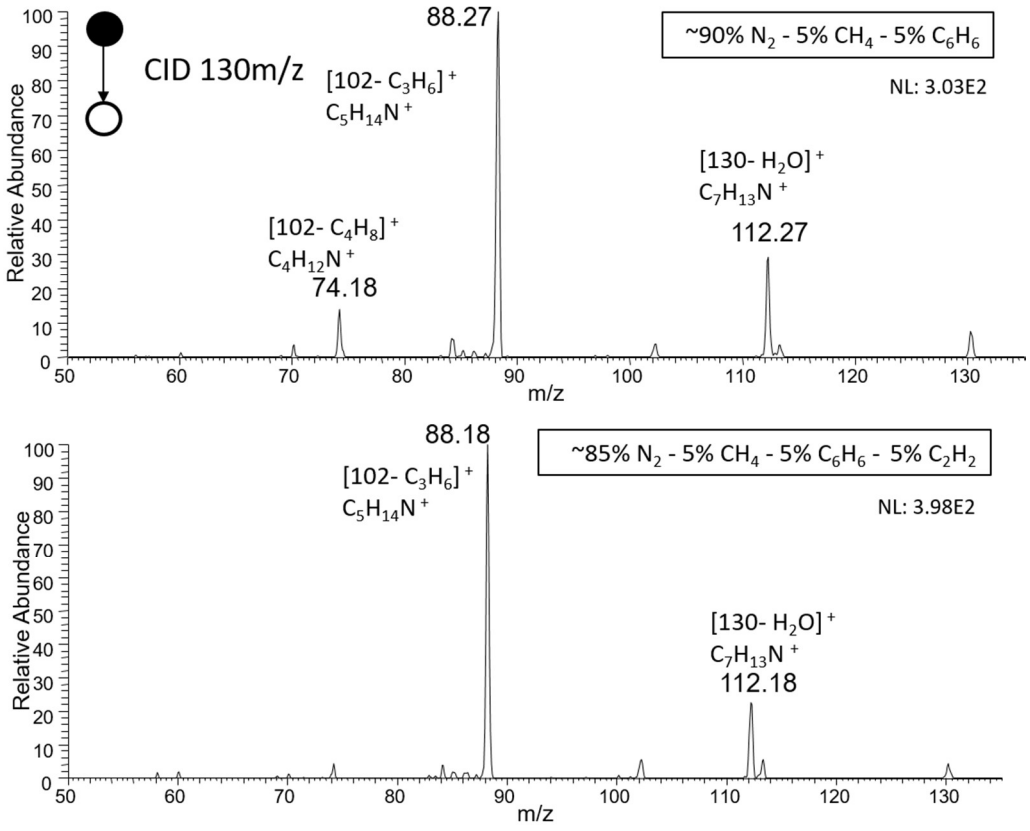

Figure 3.11. CID spectra of the 130 m/z DART peak for the benzene-doped samples from top to bottom: 90-5-5 N_2-CH_4-C_6H_6 (benzene) and 86-5-4-5 N_2-CH_4-C_2H_2-C_6H_6 (acetylene and benzene). Overall intensity is reported for each spectrum as the normalized target level (NL).

The first peak to be analyzed with this method was 130 m/z, shown in figure 3.11. This peak was observed only in the benzene doped (90-5-5) and acetylene and benzene doped (86-5-4-5) samples, and was a more abundant peak in the overall spectrum for the former. Both CID spectra show evidence for a water adduct at 112 m/z. After evaluating different possible formulae, $C_7H_{13}N$ gives the greatest number of likely isomers. Because no peaks

due to a 17 Da loss (like the ones observed in the 114 m/z CID spectra) were observed in the 130 m/z CID spectra, it was concluded that the parent molecule(s) did not contain a primary amine. This leaves a secondary amine, tertiary amine or a nitrile group as possible functional groups present in structures for the 130 m/z molecule, which are all reasonable since IR bands corresponding to secondary amines and nitriles have been observed for both these samples. Higher sensitivity would be necessary to perform subsequent CID and obtain an exact identification.

The other major fragment ion in both samples is 88 m/z, corresponding to a loss of C_3H_6 or C_2H_4N from 130 m/z. Taking these losses into account and considering the stable isomers for which one of these two losses are possible, the most likely possibility appears to be the loss of C_3H_6 from $C_8H_{19}N$. This would correspond to a secondary amine, likely comparable to the loss observed in the CID analysis of the 74 m/z DART peak, but there are too many isomers to make an exact structural identification.

The interesting aspect of the two identifications (resulting from the 112 m/z and 88 m/z fragments) is that neither formula is indicative of aromatic constituents, even though 130 m/z is not observed unless benzene is present in the gas mixture. The small amount of 130 m/z species still observed in the CID suggests that there may be some stable aromatic compounds present, but those cannot be confirmed due to the lack of CID fragmentation peaks. Non-aromatic compounds within 130 m/z suggests that the presence of benzene within the initial mixture can induce different chemical pathways, similar to the mechanism proposed for pyridine, that do not always result in aromatic compounds. The complexity of the different chemical pathways caused by the inclusion of these dopants indicates that

microenvironments and concentration gradients for molecules such as benzene need to be taken into account for more complex mechanisms in Titan's atmosphere.

3.4.4.7 147 m/z CID analysis

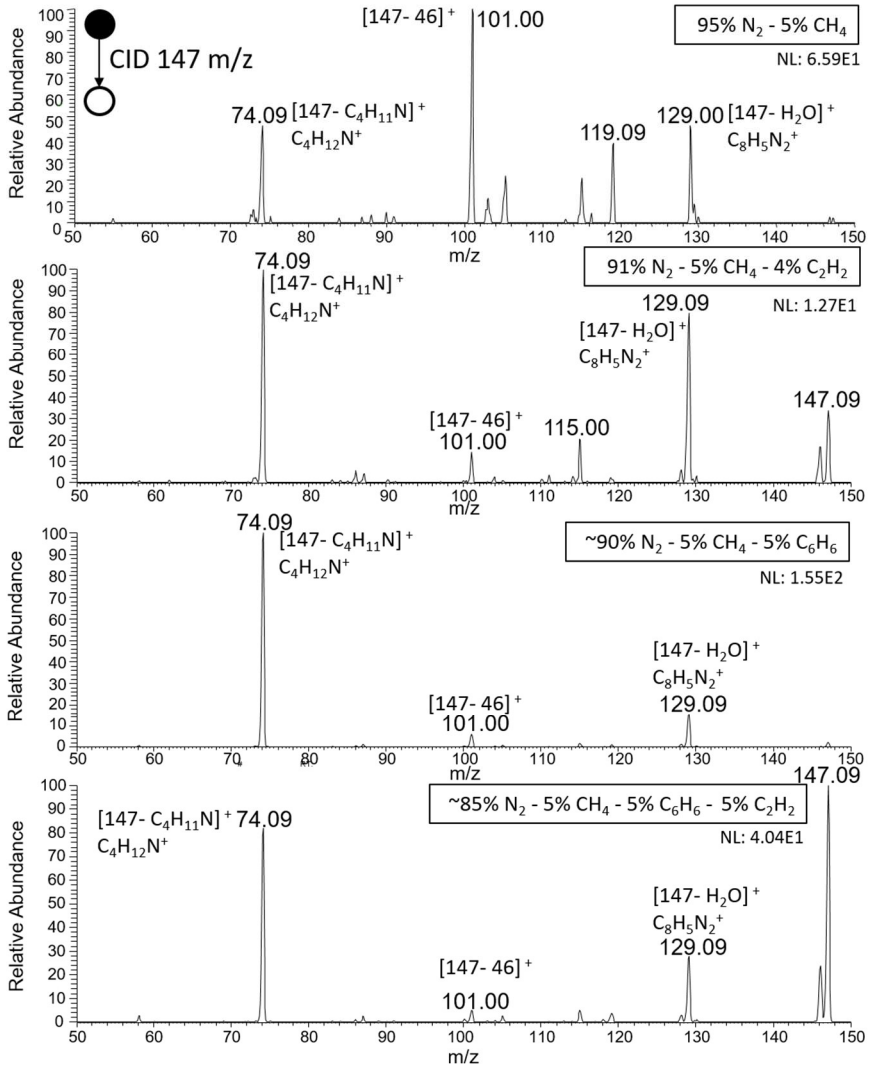

Figure 3.12. CID spectra of the 147 m/z DART peak for the four THS samples, from top to bottom: 95-5 N2-CH4, 91-5-4 N2-CH4-C2H2 (acetylene), 90-5-5 N2-CH4-C6H6 (benzene), 86-5-4-5 N2-CH4-C2H2-C6H6 (acetylene and benzene). Major fragments and losses are labeled. Overall intensity is reported for each spectrum as the normalized target level (NL).

CID spectra for the 147 m/z DART were acquired for all four samples, and are shown in figure 3.12. For all four THS samples, a fragment ion is observed at 74 m/z, which suggests that a dimer of 74 m/z, with a most likely formula of $C_4H_{11}N$, is a constituent of the 147 m/z peak. Since 74 m/z is the major peak in the overall DART spectrum for all four samples, the observation of a proton bound dimer is not surprising.

The next fragment ion investigated was 129 m/z and, due to a loss of 18 Da, was identified as a water adduct. Assignment for this species is difficult, since there are two possible formulae which would allow for stable isomers: $C_7H_{16}N_2$, in which amine isomers are abundant, and $C_8H_4N_2$, in which aromatic nitriles are the most common. Without further CID, possible assignment is based on comparison with the IR analysis of these samples. The IR data reported in Part II shows aliphatic secondary amine, C-N bond, and aromatic nitrile bands were observed for all four samples. The 129 m/z peak overall intensity is much higher in the benzene doped sample (considering the higher NL intensity for the CID spectrum), indicating that benzene is included in its synthesis as either a reactant or assisting in its production, similar to the synthesis of pyridine. Taking this into account, the $C_8H_4N_2$ formula is most likely the highest contributor to this peak, due to the aromaticity allowed by this formula and taking into account the presence of the more unique aromatic nitrile band in the IR of all four samples. The most likely compound for this formula would be dicyanobenzene, but higher sensitivity and subsequent CID will be needed in the future to confirm this identification.

In the acetylene doped (91-5-4) and acetylene and benzene doped (86-5-4-5) samples, an unfragmented 147 m/z peak is observed, suggesting a highly aromatic molecule

with little substitution, for which two likely formulae are $C_{11}H_{14}$ and $C_9H_{10}N_2$. Both of these have a high number of isomers which would not be expected to fragment, so one cannot be identified over the other. The other common peaks between the four different samples are 101 m/z and 115 m/z, with the former being the most abundant fragment for the 95-5 sample and an extremely small fragment in the other samples, and the latter being a less abundant fragment for all four samples. The losses these peaks correspond to are difficult to explain: neither 46 Da for the 101 m/z peak nor 32 Da for the 115 m/z peak have an easily identifiable loss formula. These fragment peaks thus most likely result from two-step processes, and cannot be identified without subsequent CID analysis.

The 95-5 sample displays two more fragments: 119 m/z and 105 m/z. The 119 m/z fragment is likely methylstyrene, having been identified via CID of the 119 m/z peak itself, which would likely come from the loss of ethylene from the 147 m/z parent ion. Ethylene loss from an aromatic compound similar to methylstyrene is possible, but more unfragmented parent ion would be expected in this case. The loss of methylimine from 147 m/z would better explain the fragmentation, but identification of a stable isomer for the parent formula $C_{10}H_{12}N$ is difficult, and as such an exact identification cannot be made. $C_{11}H_{14}$ can still be proposed as the most likely formula for the parent molecule though. The 105 m/z fragment, with a loss of 42 Da, would then likely be due to a loss of propene from $C_{11}H_{14}$ as well, with the fragment itself being styrene. This fits with the 119 m/z fragment belonging to methylstyrene. This does not make identification any simpler though due to the possible isomers and the same difficulties in identifying the prior 119 m/z parent. Other identifications were not attempted due to a combination of low abundance, concurrence with background CID spectra, and high number of possible isomers. Overall, the CID analysis of

the 147 m/z DART mass peak shows that with increasing mass comes increasing complexity. Many of these assignment difficulties could be addressed in the future with greater sensitivity, enabling more levels of CID analysis.

More CID spectra from these samples, reported in the SI, were not analyzed in this study due to insufficient resolution and the need for more fragmentation steps with increasing mass. The CID data reported here demonstrate the role that a dopant can play in the synthesis of unique compounds and the enhancement of the synthesis for other compounds. While initial proposals were made for many of the compounds identified here regarding synthesis, modeling studies outside the scope of this experimental study will be necessary in the future to confirm synthetic pathways and their relevance for Titan's atmosphere.

3.5 Conclusions

The Part I study demonstrated the capability of the Titan Haze Simulation (THS) experiment to probe the first and intermediate steps of Titan's atmospheric chemistry in the gas phase, and monitor the influence of dopants on the gas-phase chemistry. The Part II study performed the first analysis of the THS solid phase products with SEM and IR, identifying the aerosol growth and the many different chemical functionalities present in the material, and assessing the influence of the dopant on these parameters. Additionally, in Part II, the low temperature characteristics of the plasma were confirmed, demonstrating the THS experiment is representative of the low-temperature conditions on Titan. In this study, we have characterized the composition of the THS solid aerosols, produced in the same gas

mixtures utilized in Part II, with DART-MS, building upon the analyzes presented in Parts I and II.

The analysis performed here was the first study of a Titan simulant with DART-MS, demonstrating that the technique can be applied to the study of the solid phase aerosol products without solvation or harsh heating required by other mass spectrometric methods for solid phase analysis. The successful analysis presented here shows that DART-MS is a promising diagnostic tool for the analysis of other Titan simulants to minimize possible reactions from sample preparation methods. Further analysis of other aerosol analogues with DART-MS could allow for a better understanding of any sample changes caused by other analytical methods. The success of this analysis indicates that DART-MS and analytical methods like it should be taken into consideration for *in-situ* applications, such as future missions to Titan and other planetary bodies. The limitations in identifications due to low mass resolution and sensitivity can be addressed in future studies, for which this study will provide a foundation.

The EZ-DART-MS analysis presented here has allowed for multiple insights into the solid-phase THS simulants and their possible implications for Titan atmospheric chemistry. While these results are only applicable for molecules detectable by DART-MS, a large number of compounds were identified.

The results of these analyses show that:

— The DART spectra of the THS samples have demonstrated their surprising simplicity in composition compared to other Titan aerosol analogues for the mass range studied. While other experiments may generate aerosols from a

stochastic mixture of C, H, and N, the controlled, truncated chemistry of the THS experiment allows for the production of aerosols from specific chemical pathways, either the first steps of the N_2-CH_4 chemistry or more focused chemical processes when adding dopants to the initial N_2-CH_4 mixture. Contrary to other experiments that use continuous plasma as the energy source, the aerosol analogues produced in the THS are not overly processed in the pulsed plasma and thus could provide insight into early stage chemistry and specific chemical pathways in Titan's atmosphere.

— The simplicity of the samples was further confirmed by analysis with a higher temperature DART flow gas. The samples produced in the two simplest mixtures, N_2-CH_4 (95-5) and N_2-CH_4-C_2H_2 (91-5-4) along with the acetylene and benzene doped (86-5-4-5) sample only displayed decreased in intensity when heated as opposed to the expected higher mass species. Only the benzene doped (90-5-5) sample produced a spectrum with higher intensity for some of the peaks already detected at room temperature but no detection of heavier products, confirming the simplicity of the sample. This fits with the analysis performed in Part II showing more complex aromatic production in the benzene doped sample. This analysis at higher temperature also confirmed the ability to complete the DART analysis at room temperature allowing for DART spectra to be obtained without possible degradation from heating.

- The preservation of small molecules detectable with DART analysis indicates that these smaller semi-volatile compounds are preserved during sample collection, likely by being trapped in aerosols. Similar molecules may also be preserved on Titan in the same way during longer scale aerosol accumulation.
- The CID analysis showed several types of nitrogen incorporation, confirming similar observations in the IR analysis of Part II. The most commonly observed nitrogen-compounds in this study were amines and nitriles. The incorporation of nitriles in the Titan simulation laboratory experiment is not surprising since nitriles have been detected on Titan, but the observation of multiple amines experimentally increases the expectation for amines being present on Titan, even though they have not yet been detected there.
- The large differences in the benzene doped (90-5-5) sample compare to the other THS samples provide some interesting insights into the impact high molecular weight dopants can have on the chemistry. While the IR results indicate that it is not the most representative gas mixture for Titan aerosol analogues, the impacts benzene has on the production of different compounds as observed in the DART-MS needs to be taken into consideration. The increased production of some compounds and unique nature of the mixture could have interesting implication for benzene rich regions on Titan, considering variation of the benzene mixing ratio as well as benzene

condensation have been observed depending on altitude and seasonal variations.

The DART analysis presented here has shown the effects of particular dopants on the production, or lack thereof, of particular compounds. For example, the production of small amines is only detected in the 95-5 THS sample, indicating that other mechanisms impede their production in the presence of dopants. Another example is the much larger production of pyridine in the presence of benzene, not only providing support for a mechanism reported in other studies but also showing that these dopants have synthetic impacts beyond their direct inclusion into the observed products. These results justify future studies with other dopants and mechanistic investigations into the implications this analysis may have for Titan atmospheric chemistry.

3.6 Acknowledgements

We would like to thank Mark Smith for providing the Arizona Titan aerosol simulant sample for analysis. The research was funded by NSF award number CHE-1508825. The early part of this work was funded by NASA Astrobiology Institute, Titan as a Prebiotic Chemical System, the Keck Institute for Space Studies, Future Missions to Titan: Scientific and Engineering Challenges, and NASA SMD (SSW). K.T.U. acknowledges financial support from the Harriett Jenkins Pre-Doctoral Fellowship Program. We also thank the Caltech Glass Shop for their assistance in the fabrication of the EZ-DART source and the technical support of R. Walker and E. Quigley (NASA ARC).

3.7 References

1. C. Sagan, W. R. Thompson and B. N. Khare, *Accounts of Chemical Research*, 1992, **25**, 286-292.
2. H. B. Niemann, S. K. Atreya, J. E. Demick, D. Gautier, J. A. Haberman, D. N. Harpold, W. T. Kasprzak, J. I. Lunine, T. C. Owen and F. Raulin, *J Geophys Res-Planet*, 2010, **115**, E12006.
3. H. B. Niemann, S. K. Atreya, S. J. Bauer, G. R. Carignan, J. E. Demick, R. L. Frost, D. Gautier, J. A. Haberman, D. N. Harpold, D. M. Hunten, G. Israel, J. I. Lunine, W. T. Kasprzak, T. C. Owen, M. Paulkovich, F. Raulin, E. Raaen and S. H. Way, *Nature*, 2005, **438**, 779-784.
4. F. Raulin, *Space Science Reviews*, 2005, **116**, 471-487.
5. F. Raulin and T. Owen, *Space Science Reviews*, 2002, **104**, 377-394.
6. W. C. Maguire, R. A. Hanel, D. E. Jennings, V. G. Kunde and R. E. Samuelson, *Nature*, 1981, **292**, 683-686.
7. V. G. Kunde, A. C. Aikin, R. A. Hanel, D. E. Jennings, W. C. Maguire and R. E. Samuelson, *Nature*, 1981, **292**, 686-688.
8. F. M. Flasar, R. K. Achterberg, B. J. Conrath, P. J. Gierasch, V. G. Kunde, C. A. Nixon, G. L. Bjoraker, D. E. Jennings, P. N. Romani, A. A. Simon-Miller, B. Bézard, A. Coustenis, P. G. J. Irwin, N. A. Teanby, J. Brasunas, J. C. Pearl, M. E. Segura, R. C. Carlson, A. Mamoutkine, P. J. Schinder, A. Barucci, R. Courtin, T. Fouchet, D. Gautier, E. Lellouch, A. Marten, R. Prangé, S. Vinatier, D. F. Strobel, S. B. Calcutt, P. L. Read, F. W. Taylor, N. Bowles, R. E. Samuelson, G. S. Orton, L. J. Spilker, T. C. Owen, J. R.

Spencer, M. R. Showalter, C. Ferrari, M. M. Abbas, F. Raulin, S. Edgington, P. Ade and E. H. Wishnow, *Science*, 2005, **308**, 975-978.

9. M. L. Cable, S. M. Hörst, R. Hodyss, P. M. Beauchamp, M. A. Smith and P. A. Willis, *Chemical Reviews*, 2012, **112**, 1882-1909.
10. F. Raulin, C. Brasse, O. Poch and P. Coll, *Chemical Society Reviews*, 2012, **41**, 5380-5393.
11. M. Fulchignoni, F. Ferri, F. Angrilli, A. J. Ball, A. Bar-Nun, M. A. Barucci, C. Bettanini, G. Bianchini, W. Borucki, G. Colombatti, M. Coradini, A. Coustenis, S. Debei, P. Falkner, G. Fanti, E. Flamini, V. Gaborit, R. Grard, M. Hamelin, A. M. Harri, B. Hathi, I. Jernej, M. R. Leese, A. Lehto, P. F. Lion Stoppato, J. J. Lopez-Moreno, T. Makinen, J. A. M. McDonnell, C. P. McKay, G. Molina-Cuberos, F. M. Neubauer, V. Pirronello, R. Rodrigo, B. Saggin, K. Schwingenschuh, A. Seiff, F. Simoes, H. Svedhem, T. Tokano, M. C. Towner, R. Trautner, P. Withers and J. C. Zarnecki, *Nature*, 2005, **438**, 785-791.
12. S. M. Hörst, *Journal of Geophysical Research: Planets*, 2017, **122**, 432-482.
13. E. Sciamma-O'Brien, N. Carrasco, C. Szopa, A. Buch and G. Cernogora, *Icarus*, 2010, **209**, 704-714.
14. N. Sarker, A. Somogyi, J. I. Lunine and M. A. Smith, *Astrobiology*, 2003, **3**, 719-726.
15. H. Imanaka, B. N. Khare, J. E. Elsila, E. L. O. Bakes, C. P. McKay, D. P. Cruikshank, S. Sugita, T. Matsui and R. N. Zare, *Icarus*, 2004, **168**, 344-366.
16. C. He, G. Lin, K. T. Upton, H. Imanaka and M. A. Smith, *The Journal of Physical Chemistry A*, 2012, **116**, 4760-4767.
17. H. Imanaka and M. A. Smith, *Geophysical Research Letters*, 2007, **34**.

18. H. Imanaka and M. A. Smith, *Proceedings of the National Academy of Sciences*, 2010, **107**, 12423-12428.

19. R. Thissen, V. Vuitton, P. Lavvas, J. Lemaire, C. Dehon, O. Dutuit, M. A. Smith, S. Turchini, D. Catone, R. V. Yelle, P. Pernot, A. Somogyi and M. Coreno, *The Journal of Physical Chemistry A*, 2009, **113**, 11211-11220.

20. B. Cunha de Miranda, G. A. Garcia, F. Gaie-Levrel, A. Mahjoub, T. Gautier, B. Fleury, L. Nahon, P. Pernot and N. Carrasco, *The Journal of Physical Chemistry A*, 2016, **120**, 6529-6540.

21. C. Szopa, G. Cernogora, L. Boufendi, J. J. Correia and P. Coll, *Planetary and Space Science*, 2006, **54**, 394-404.

22. G. Alcouffe, M. Cavarroc, G. Cernogora, F. Ouni, A. Jolly, L. Boufendi and C. Szopa, *Plasma Sources Sci T*, 2010, **19**.

23. N. Carrasco, F. Jomard, J. Vigneron, A. Etcheberry and G. Cernogora, *Planetary and Space Science*, 2016, **128**, 52-57.

24. E. Sciamma-O'Brien, C. L. Ricketts and F. Salama, *Icarus*, 2014, **243**, 325-336.

25. E. Sciamma-O'Brien, K. T. Upton and F. Salama, *Icarus*, 2017, **289**, 214-226.

26. A. Somogyi, C. H. Oh, M. A. Smith and J. I. Lunine, *Journal of the American Society for Mass Spectrometry*, 2005, **16**, 850-859.

27. A. Somogyi, M. A. Smith, V. Vuitton, R. Thissen and I. Komaromi, *Int J Mass Spectrom*, 2012, **316**, 157-163.

28. A. Somogyi, R. Thissen, F. R. Orthous-Daunay and V. Vuitton, *Int J Mol Sci*, 2016, **17**.

29. M. C. Pietrogrande, P. Coll, R. Sternberg, C. Szopa, R. Navarro-Gonzalez, C. Vidal-Madjar and F. Dondi, *Journal of Chromatography A*, 2001, **939**, 69-77.

30. M. Morisson, C. Szopa, N. Carrasco, A. Buch and T. Gautier, *Icarus*, 2016, **277**, 442-454.

31. M. E. Monge and F. M. Fernandez, in *Ambient Ionization Mass Spectrometry*, The Royal Society of Chemistry, 2015, DOI: 10.1039/9781782628026-00001, pp. 1-22.

32. M. E. Monge, G. A. Harris, P. Dwivedi and F. M. Fernandez, *Chem Rev*, 2013, **113**, 2269-2308.

33. X. Ding and Y. Duan, *Mass Spectrometry Reviews*, 2015, **34**, 449-473.

34. W. Romão, L. V. Tose, B. G. Vaz, S. G. Sama, R. Lobinski, P. Giusti, H. Carrier and B. Bouyssiere, *Journal of The American Society for Mass Spectrometry*, 2016, **27**, 182-185.

35. K. A. Schilling Fahnestock, L. D. Yee, C. L. Loza, M. M. Coggon, R. Schwantes, X. Zhang, N. F. Dalleska and J. H. Seinfeld, *The Journal of Physical Chemistry A*, 2015, **119**, 4281-4297.

36. M. N. Chan, T. Nah and K. R. Wilson, *Analyst*, 2013, **138**, 3749-3757.

37. R. B. Cody, J. A. Laramée and H. D. Durst, *Analytical Chemistry*, 2005, **77**, 2297-2302.

38. L. Song, S. C. Gibson, D. Bhandari, K. D. Cook and J. E. Bartmess, *Analytical Chemistry*, 2009, **81**, 10080-10088.

39. R. B. Cody, *Analytical Chemistry*, 2009, **81**, 1101-1107.

40. R. B. Cody and A. J. Dane, *Journal of The American Society for Mass Spectrometry*, 2013, **24**, 329-334.

41. K. Upton, K. Schilling and J. Beauchamp, *Analytical Methods*, 2017, **9**, 5065-5074.

42. B. H. P. Broks, W. J. M. Brok, J. Remy, J. J. A. M. van der Mullen, A. Benidar, L. Biennier and F. Salama, *Physical Review E*, 2005, **71**, 036409.

43. L. Biennier, A. Benidar and F. Salama, *Chemical Physics*, 2006, **326**, 445-457.

44. A. R. Johnson and E. E. Carlson, *Analytical Chemistry*, 2015, **87**, 10668-10678.

45. Vinatier S. et. al., *Icarus*, submitted.

46. J. H. Gross, *Analytical and Bioanalytical Chemistry*, 2014, **406**, 63-80.

47. P. Ehrenfreund, J. J. Boon, J. Commandeur, C. Sagan, W. R. Thompson and B. Khare, *Adv Space Res*, 1994, **15**, 335-342.

48. E. H. Wilson and S. K. Atreya, *Planetary and Space Science*, 2003, **51**, 1017-1033.

49. Z. Zhang, X. Gong, S. Zhang, H. Yang, Y. Shi, C. Yang, X. Zhang, X. Xiong, X. Fang and Z. Ouyang, *Scientific Reports*, 2013, **3**, 3481.

50. D. S. N. Parker, R. I. Kaiser, O. Kostko, T. P. Troy, M. Ahmed, B.-J. Sun, S.-H. Chen and A. H. H. Chang, *Physical Chemistry Chemical Physics*, 2015, **17**, 32000-32008.

51. M. Cordiner, M. Y Palmer, C. A. Nixon, S. B. Charnley, M. J. Mumma, P. G. J. Irwin, N. A. Teanby, Z. Kisiel and J. Serigano, 2015.

52. V. Vuitton, R. V. Yelle and J. Cui, *Journal of Geophysical Research: Planets*, 2008, **113**, E05007.

53. Y. Sekine, S. Lebonnois, H. Imanaka, T. Matsui, E. L. O. Bakes, C. P. McKay, B. N. Khare and S. Sugita, *Icarus*, 2008, **194**, 201-211.

54. Q. Wu, H. Shi, Y. Ma, C. Adams, T. Eichholz, T. Timmons and H. Jiang, *Talanta*, 2015, **131**, 736-741.

55. A. Belloche, K. M. Menten, C. Comito, H. S. P. Müller, P. Schilke, J. Ott, S. Thorwirth and C. Hieret, *A&A*, 2008, **482**, 179-196.

56. J. C. Loison, E. Hébrard, M. Dobrijevic, K. M. Hickson, F. Caralp, V. Hue, G. Gronoff, O. Venot and Y. Bénilan, *Icarus*, 2015, **247**, 218-247.

57. N. Balucani, F. Leonori, R. Petrucci, M. Stazi, D. Skouteris, M. Rosi and P. Casavecchia, *Faraday Discussions*, 2010, **147**, 189-216.

58. A. M. Hamid, P. P. Bera, T. J. Lee, S. G. Aziz, A. O. Alyoubi and M. S. El-Shall, *The Journal of Physical Chemistry Letters*, 2014, **5**, 3392-3398.

59. Y. A. Jeilani, C. Fearce and M. T. Nguyen, *Physical Chemistry Chemical Physics*, 2015, **17**, 24294-24303.

60. A. Mess, J. P. Vietzke, C. Rapp and W. Francke, *Anal Chem*, 2011, **83**, 7323-7330.

3.8 Supplemental Information

3.8.1 CID Spectra of 80 m/z

The CID spectra from the 90-5-5 N_2-CH_4-C_6H_6 (benzene) sample and neat pyridine are shown below. Both display the reaction product with water as the only peak.

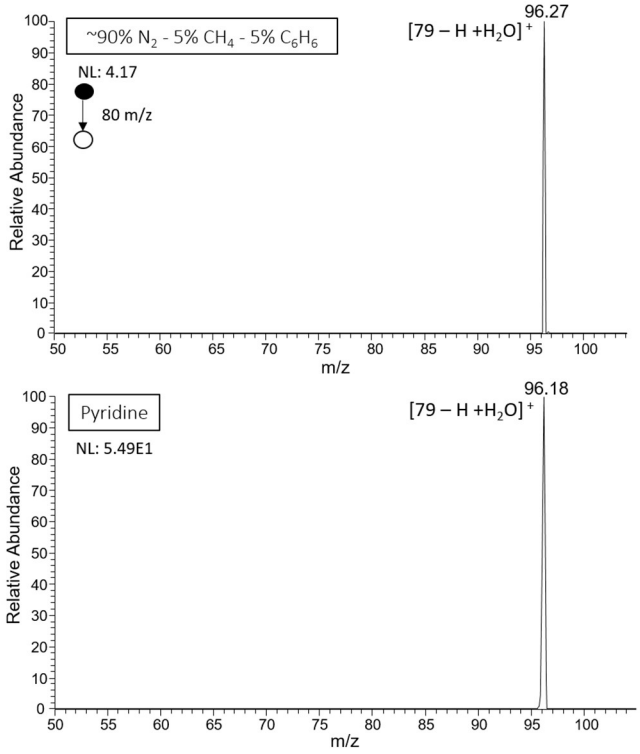

Figure 3.13. Top: Spectrum for the CID of 80 m/z from the 90-5-5 N_2-CH_4-C_6H_6 (benzene) sample. Bottom: Spectrum for the CID of 80 m/z from neat pyridine. Overall intensity is reported for each spectrum as the normalized target level (NL).

3.8.2 CID Spectra of 173 m/z and Discussion

The fragments from 173 m/z are more complicated, since the losses seems to suggest two very different molecular formula making up the peak. The fragment as 113 m/z is from a loss of $C_2H_8N_2$ and is suggestive of the complex formula $C_8H_{20}N_4$. While high degrees of

nitrogenation for these molecules is not impossible, it would be unlikely to be favored due to low stability. Even though this species produces the base fragment for 173 m/z, the fact that the parent ion is in low abundance for all four samples increases the support for this formula. The C_2H_4 and C_3H_6 losses are suggestive of $C_{10}H_{23}N_2$, due in part to the high number of isomers that could enable those losses.

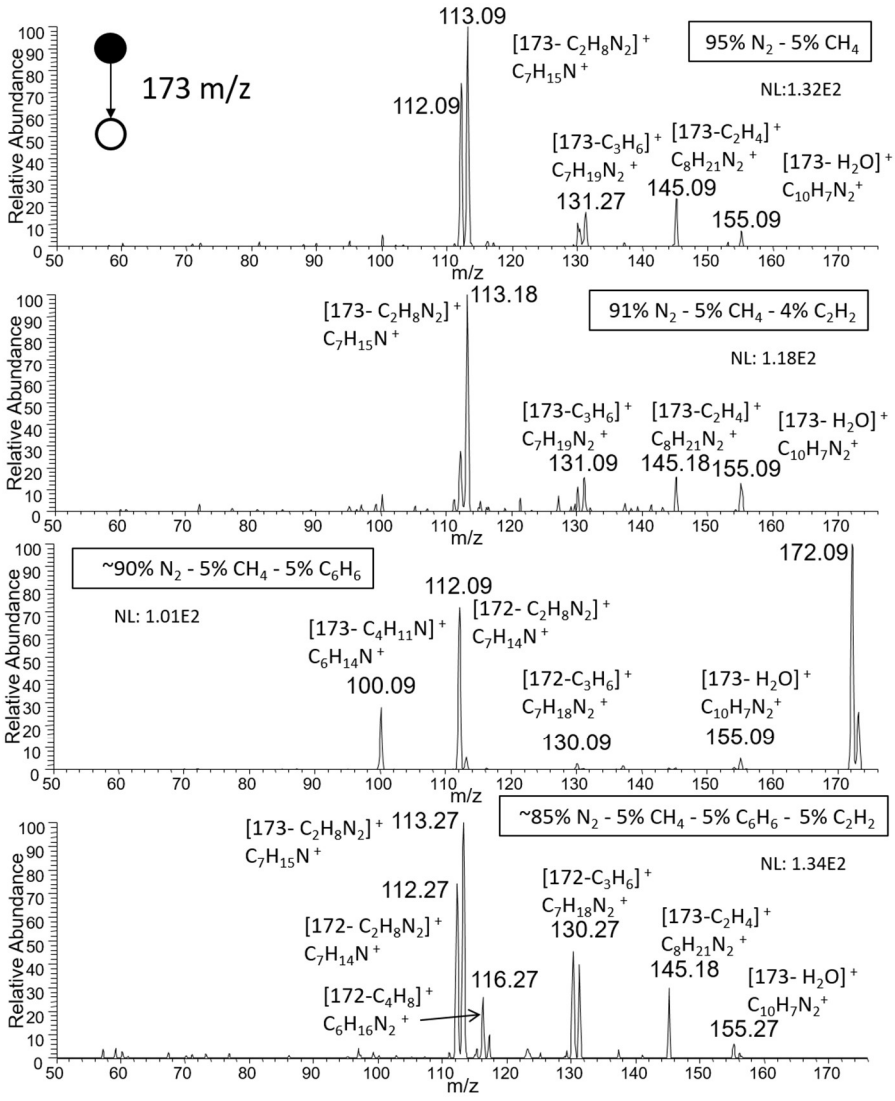

Figure 3.14. The CID of 173 m/z for each sample going, from top to bottom : 95-5 N_2-CH_4, 91-5-4 N_2-CH_4-C_2H_2 (acetylene), 90-5-5 N_2-CH_4-C_6H_6 (benzene), 86-5-4-5 N_2-CH_4-C_2H_2-C_6H_6 (acetylene and benzene). Major fragments and losses are labeled. Overall intensity is reported for each spectrum as the normalized target level (NL).

3.8.3 Spectra without background subtraction and background spectra for each sample

Shown below are all the spectra used for background subtraction and their respective spectra prior to subtraction. The subtraction was performed with the Xcalibur software suite.

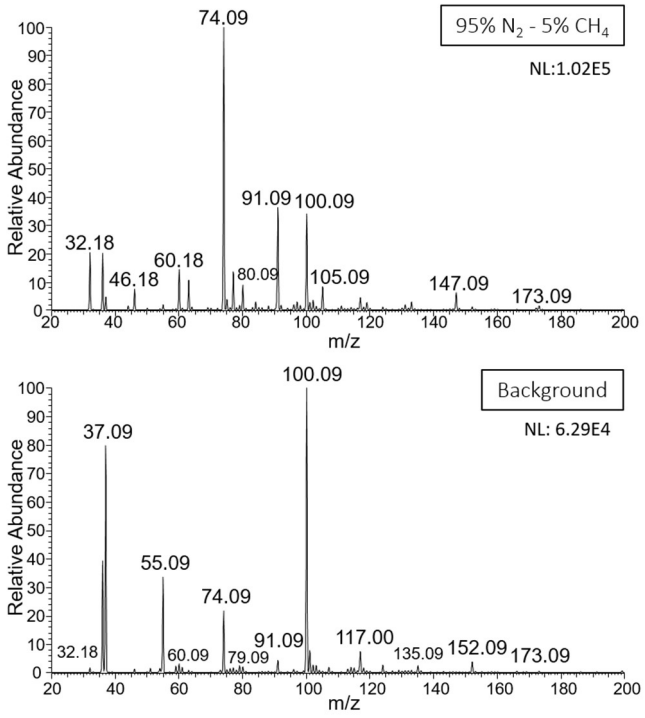

Figure 3.15. Top: Spectrum for the 95-5 N_2-CH_4 sample without background subtraction. Bottom: Background spectrum used for subtraction from the 95-5 N_2-CH_4 spectrum. Overall intensity is reported for each spectrum as the normalized target level (NL).

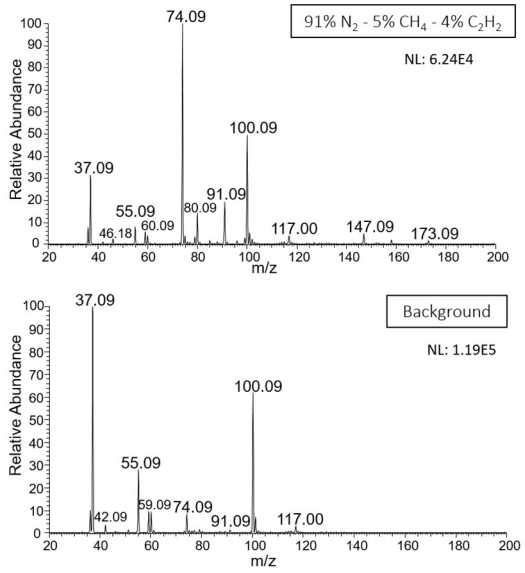

Figure 3.16. Top: Spectrum for the 91-5-4 N_2-CH_4-C_2H_2 (acetylene) sample without background subtraction. Bottom: Background spectrum used for subtraction from the 91-5-4 N_2-CH_4-C_2H_2 (acetylene) spectrum. Overall intensity is reported for each spectrum as the normalized target level (NL).

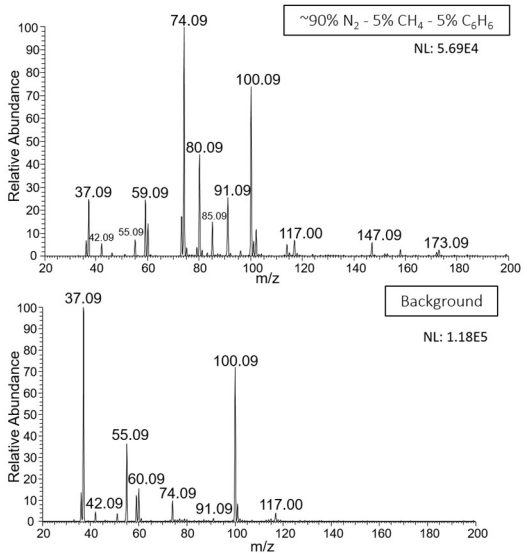

Figure 3.17. Top: Spectrum for the 90-5-5 N_2-CH_4-C_6H_6 (benzene) sample without background subtraction. Bottom: Background spectrum used for subtraction from the 90-5-5 N_2-CH_4-C_6H_6 (benzene) spectrum. Overall intensity is reported for each spectrum as the normalized target level (NL).

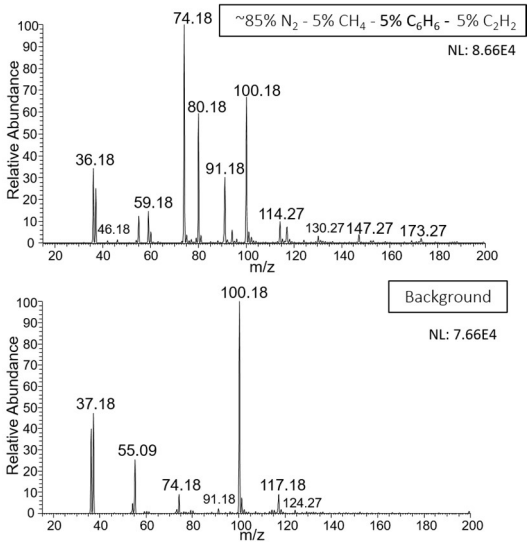

Figure 3.18. Top: Spectrum for the 86-5-4-5 N_2-CH_4-C_2H_2-C_6H_6 (acetylene and benzene) sample without background subtraction. Bottom: Background spectrum used for subtraction from the 86-5-4-5 N_2-CH_4-C_2H_2-C_6H_6 (acetylene and benzene) spectrum. Overall intensity is reported for each spectrum as the normalized target level (NL).

3.8.4 CID of studied peaks from atmospheric background

The figures below show CID of peaks from an atmospheric background taken after the original samples and background were acquired. If any similarities to peaks from CID of the same peaks in the sample are seen, any peaks analyzed for the sample were higher in intensity. All background CID were acquired under the same conditions used for the samples. CID of 80 m/z in atmospheric background produced no fragments. Overall intensity is reported for each spectrum as the normalized target level (NL).

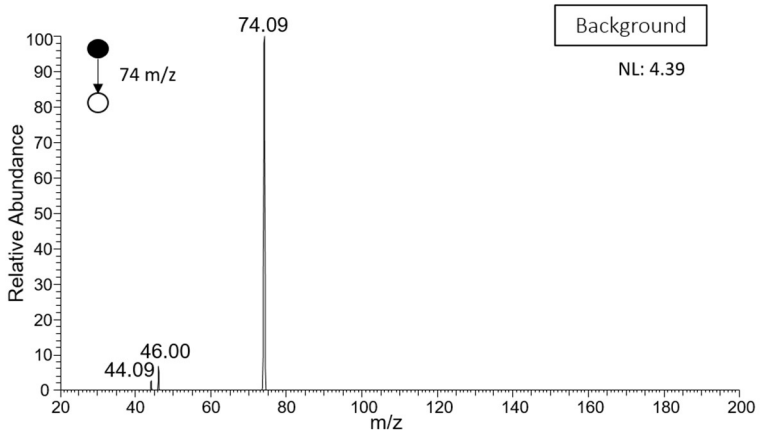

Figure 3.19. CID of the 74 m/z present in atmospheric background.

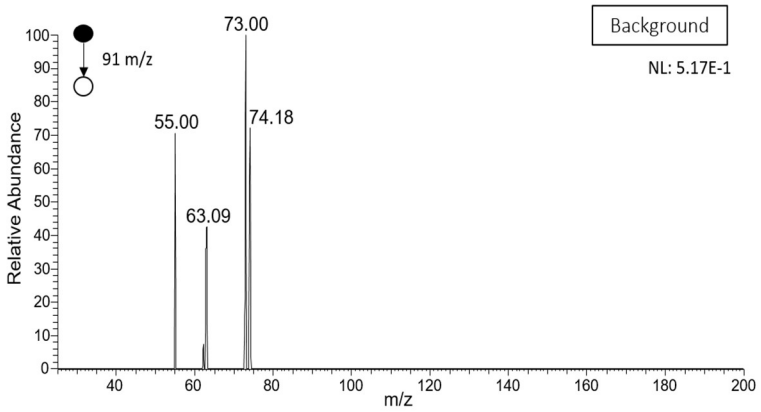

Figure 3.20. CID of the 91 m/z present in atmospheric background.

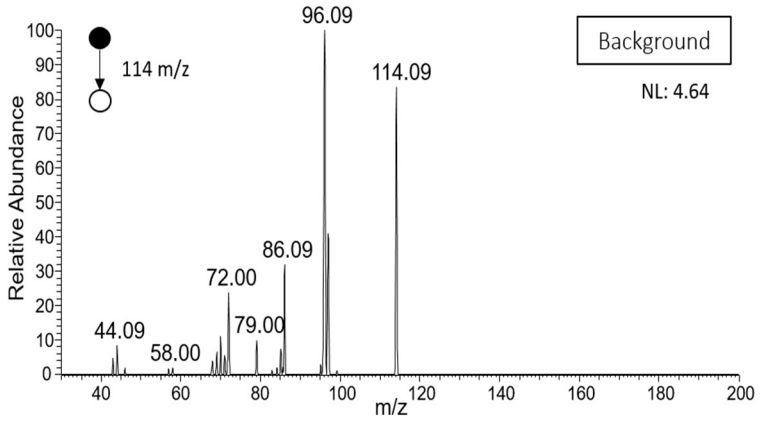

Figure 3.21. CID of the 114 m/z present in atmospheric background.

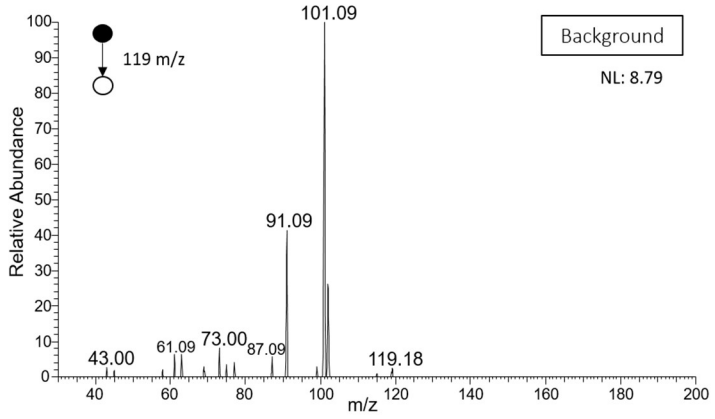

Figure 3.22. CID of the 119 m/z present in atmospheric background.

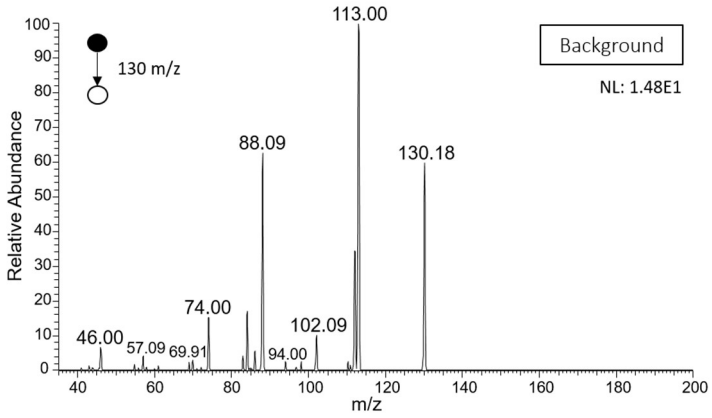

Figure 3.23. CID of the 130 m/z present in atmospheric background.

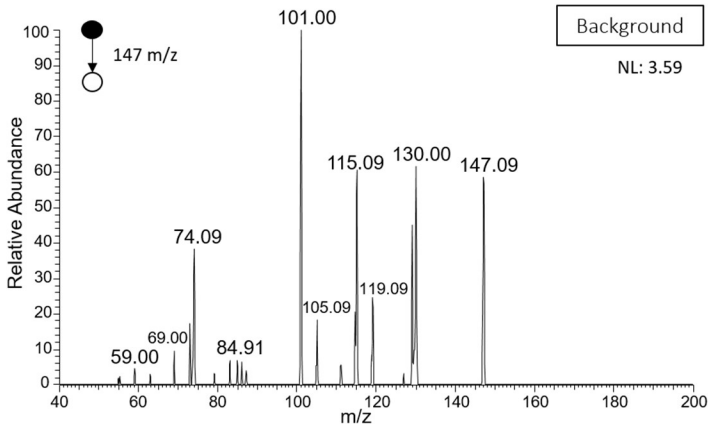

Figure 3.24. CID of the 147 m/z present in atmospheric background.

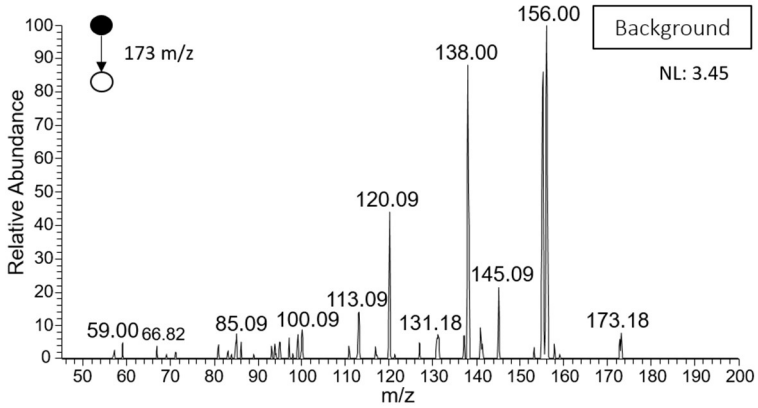

Figure 3.25. CID of the 173 m/z present in atmospheric background.